NATIONAL ADVISORY COMMITTEE FOR AERONAUTICS

TECHNICAL NOTE 1941

ATTAINABLE CIRCULATION OF AIRFOILS IN CASCADE

By Arthur W. Goldstein and Artur Mager

Lewis Flight Propulsion Laboratory
Cleveland, Ohio

Washington
September 1949

NATIONAL ADVISORY COMMITTEE FOR AERONAUTICS

TECHNICAL NOTE 1941

ATTAINABLE CIRCULATION OF AIRFOILS IN CASCADE

By Arthur W. Goldstein and Artur Mager

SUMMARY

From consideration of available information on boundary-layer behaviour, a relation among profile thickness, maximum surface velocity, Reynolds number, velocity diagram, and solidity is established for a cascade of airfoils immersed in a two-dimensional incompressible fluid flow. Several cascades are computed to show the effect of various cascade design parameters on minimum required cascade solidity. Comparisons with experimentally determined blade performance show that the derived blade loadings are equal or higher for moderate flow deceleration and somewhat lower for large deceleration. Blades with completely laminar flow appear practical for impulse or reaction blading.

INTRODUCTION

In the design of compressor and turbine blading, the choice of blade sections and spacing is usually made on the basis of experimental results from several cascades. An enormous amount of data is required to cover the entire range of inlet and outlet angles, Reynolds numbers, blade sections, spacings, and maximum surface velocities.

The relations among the blade circulation and its thickness, Reynolds number, maximum surface velocity, and spacing were determined at the NACA Lewis laboratory in a qualitative fashion for two-dimensional, incompressible flow. This problem has been studied empirically (references 1 and 2) without any attempt to relate the problem to the basic determining factor - the boundary layer. The analysis presented herein establishes such a relation on a more rational basis.

As the gas flows through a cascade of airfoils, on the suction surface of a blade the inlet velocity is raised to some maximum local value and then decreased until, near the trailing edge, its value is in the neighborhood of the exit velocity. A blade cascade will operate in a compressible fluid with less likelihood of local

shocks, resultant losses, and choking if the design is such that the maximum surface velocity is maintained as low as possible. The preassigned, low maximum surface velocity should extend over as large a portion of the suction surface as possible before diffusion in order to raise the circulation to a maximum. Because the velocity must decrease near the trailing edge from its maximum value to a value close to the exit velocity, the maximum possible rate of diffusion will, in effect, determine the arc length on which the suction-surface velocity is kept at its maximum. The blade circulation attainable is then determined by the maximum diffusion rate possible.

In dealing with incompressible flow, the same general type of velocity distribution is specified herein, and the diffusion rate is determined by several conditions to avoid separation of flow from the blade surface. Once the possible velocity distribution on the suction surface is determined, an approximate computation is then used with a specified velocity diagram and blade thickness to compute the pressure-surface-velocity distribution, blade circulation, and spacing.

The results reported herein are not to be interpreted as giving an exact velocity distribution of airfoil sections for application. In the first place, the assumption of no separation in some cases reduces obtainable lift and increases the blade solidity and the surface for friction, which increases skin friction loss. If a small region of separated flow is permitted, the increase in form drag may be insufficient to increase total drag in view of the increase in blade lift and decrease in blade number and skin friction. Another limitation is possible in applicability of the boundary-layer equations used in prescribing the suction-surface-velocity distribution. The velocities deduced from these equations are not conventional in that the form factor of the boundary layer (ratio of displacement to momentum thickness) rapidly rises to the maximum permissible value and then remains nearly constant; whereas with conventional velocity distributions, it slowly increases and then very rapidly rises near the separation region. Thus the empirical equations describing the development of the boundary-layer form factor may not be accurately applicable for such velocity distributions. In order to demonstrate the several solutions that might be applicable, the surface velocities were prescribed according to three rules. Garner's equations (reference 3) were used with the form factor first rising rapidly and then remaining nearly constant with limiting values of either 1.85 or 2.14. Also a diffusion rate was chosen equal to 0.885 of the value prescribed by Kalikhman (reference 4) for separation.

A final consideration lies in the approximate nature of the procedure for computing the lower surface-velocity distribution. In this process, the effect of thickness is assumed to result in a surface-velocity component, which varies as a second-degree parabolic function of the surface arc length. Consequently, the results apply to a special family of thickness distributions, which may not be the optimum for the prescribed suction-surface-velocity distribution. Moreover, the estimate of the effect of thickness is inexact so that the estimate of the airfoil-thickness distribution will differ somewhat from the actual thickness of an airfoil with the prescribed surface velocities.

Although the absolute values of blade circulations are inexact, some very definite trends are nevertheless demonstrated, particularly with respect to maximum surface velocity, Reynolds number, and blade thickness.

SELECTION OF VELOCITY DISTRIBUTION ON SUCTION SURFACE OF BLADE

General Considerations

As mentioned in the Introduction, the velocity distribution on the suction surface to be investigated will consist of a velocity that is supposed to rise to its maximum value in a negligibly short distance from the leading-edge stagnation point and to maintain that value as far back along the airfoil as possible. The velocity must then decrease from the maximum value to the value near the trailing edge that differs slightly from the downstream velocity. A deceleration with a maximum safe velocity gradient without flow separation between the maximum velocity and a final velocity is required. In order to find the suction-surface-velocity distribution, it is necessary to investigate the development of the boundary layer, which determines the allowable rate of diffusion. The general shape of the velocity-distribution curves is shown in figure 1, which also indicates some of the nomenclature. (All symbols used are defined in appendix A.)

Laminar Boundary Layer

Region of constant velocity. - For the region of constant velocity $U(x) = U_{max}$, the equation for the momentum thickness of the laminar boundary layer is

$$\theta = 0.664\sqrt{\frac{\nu x}{U_{max}}} \tag{1}$$

where

θ momentum thickness of boundary layer

ν kinematic viscosity of gas

x arc length on airfoil suction surface

U suction-surface velocity just outside boundary layer

The subscript max indicates maximum value of surface velocity. The Reynolds number of the boundary layer based on momentum thickness is defined as

$$R \equiv U\theta/\nu \tag{2}$$

The form factor H is defined as

$$H \equiv \delta^*/\theta \tag{3}$$

where δ^* is the displacement thickness of the boundary layer. In the region of constant velocity, H = 2.614.

Region of diffusion. - For diffusion with a laminar boundary layer, the approximate method of Loitsianskii (reference 5) was used. According to that system of equations, separation will occur if the proportional change in velocity dU/U per unit of arc length dx equal to the generalized momentum thickness L reaches a value of -0.08884. That is

$$D_L \equiv \frac{L}{U}\frac{dU}{dx} \tag{4}$$

where

$$L \equiv \theta R = \theta^2 \frac{U}{\nu} \tag{5}$$

must be greater than -0.08884. A value of D_L = -0.06618 was arbitrarily selected to give a high diffusion rate without introducing laminar separation. Loitsianskii's equation for boundary-layer growth then becomes

$$\frac{1}{U}\frac{dU}{dx} = \frac{-\frac{D_L}{F}\left(\frac{d^2U}{dx^2}\right)}{\left(\frac{dU}{dx}\right)}$$

where F, a function of D_L, is a constant equal to 0.8517 for $D_L = -0.06618$.

This equation is integrated to give

$$\frac{dU}{dx} = KU^{-F/D_L}$$

By substituting for dU/dx from the definition of D_L, the constant of integration K is evaluated to give

$$\frac{U}{U_l} = \left(\frac{L}{L_l}\right)^{\frac{D_L}{D_L+F}} = \left(\frac{L}{L_l}\right)^{-0.08425} \tag{6a}$$

where the subscript l indicates the value at the beginning of the laminar diffusion process. By differentiating equation (6a) and eliminating dU/U by means of equation (4), there is obtained

$$D_L\frac{dx}{L} = \frac{dU}{U} = \frac{D_L}{D_L+F}\frac{dL}{L}$$

which is integrated to

$$\frac{L}{L_l} = 1 + (D_L+F)\left(\frac{x - x_l}{L_l}\right) = 1 + 0.7855\left(\frac{x - x_l}{L_l}\right) \tag{6b}$$

Equations (1) and (5) are used to relate the constants x_l and L_l

$$L_l = 0.441\, x_l$$

From equation (5)

$$\frac{L}{L_l} = \frac{\theta}{\theta_l}\frac{R}{R_l} = \left(\frac{\theta}{\theta_l}\right)^2\frac{U}{U_l}$$

or

$$\frac{\theta}{\theta_l} = \left(\frac{L}{L_l}\frac{U_l}{U}\right)^{\frac{1}{2}} = \left(\frac{L}{L_l}\right)^{\frac{F}{2(F+D_L)}} = \left(\frac{L}{L_l}\right)^{0.5421} \tag{6c}$$

also

$$\frac{R}{R_l} = \left(\frac{L}{L_l}\right)^{\frac{F+2D_L}{2(F+D_L)}} = \left(\frac{L}{L_l}\right)^{0.4579} \tag{6d}$$

The velocity potential φ, defined by

$$\varphi \equiv \int_0^x U dx$$

is found from

$$\frac{\varphi - \varphi_l}{L_l\ U_l} = \frac{1}{L_l\ U_l}\int_{x_l}^{x} U dx = \frac{1}{F+2D_L}\left[\left(\frac{L}{L_l}\right)^{\frac{F+2D_L}{F+D_L}} - 1\right] = 1.390\left[\left(\frac{L}{L_l}\right)^{0.9158} - 1\right] \tag{6e}$$

The constant $\varphi_l/U_l\ L_l$ is computed from the equations for the nondiffusing section giving

$$\frac{\varphi_l}{U_l\ L_l} = 2.268 \tag{6f}$$

The form factor of the boundary layer H in the region $D_L = -0.06618$ has a value of 3.214 (reference 5).

In applications, it is convenient to know the position x_l in percent of the total length of the suction surface X. From equation (6b),

$$\frac{X}{L_l} = \frac{x_l}{L_l} + \frac{1}{F+D_L}\left(\frac{L_f}{L_l} - 1\right) \tag{7}$$

The subscript f applies to the final value at the trailing edge of the blade. In terms of velocities, with $\frac{x_l}{L_l} = \frac{1}{0.441}$,

$$\frac{X}{L_l} = 2.268\left(\frac{1}{F+D_L}\right)\left[\left(\frac{U_f}{U_l}\right)^{\frac{F+D_L}{D_L}} - 1\right] \tag{7a}$$

Then

$$\frac{x_l}{X} = \frac{1}{1 + \frac{0.441}{F+D_L}\left[\left(\frac{U_f}{U_l}\right)^{\frac{F+D_L}{D_L}} - 1\right]} \tag{8}$$

In figure 2, the variation of U/U_l and R/R_l with $x-x_l/L_l$ is shown for diffusion with the laminar boundary layer. In applying these curves for any airfoil, the scale of the diffusing region must be adjusted for the value of L_l that is equal to $0.441\ x_l$. In figure 3, the curve for the entire suction-surface potential is shown with X as the unit of length rather than L_l.

Transition

As the air flows over the blade surface, the thickness of the laminar boundary layer will increase until a point is reached where the character of the boundary-layer flow will change from laminar to turbulent. The boundary layer will then develop according to different laws and will therefore also sustain a different pressure gradient without separation.

Transition occurs at a certain value of R_{tr}, which will depend on the turbulence intensity and scale, the pressure gradient, the roughness and the curvature of the surface, and on heat transfer through the boundary layer. An R_{tr} value of 250 has been selected

for this analysis in consideration of the high level of free-stream turbulence in turbomachinery, which tends to reduce R_{tr} to a low value. According to Gruschwitz (reference 6), observed boundary layers were always laminar if $R < 250$ regardless of the intensity of free-stream turbulence, and turbulent boundary layers have been observed for $R > 250$. Gruschwitz neglects to mention the pressure gradient at which these observations were made and as a consequence the assumption $R_{tr} = 250$ might be somewhat low for flows with zero pressure gradient. It should be noted that if for any reason transition is delayed so that the rapid diffusion rate prescribed for a turbulent boundary layer is applied to a laminar layer, separation results. On the other hand, the effect of pressure gradient is to reduce markedly the value of R_{tr}, so that even should the transition be delayed in the zero pressure-gradient region it will probably occur at the inception of the diffusion process.

Turbulent Boundary Layer

The momentum equation for the boundary layer is

$$\frac{d\theta}{dx} + \frac{\theta}{U}\frac{dU}{dx}(2+H) = \frac{\tau}{\rho U^2} \tag{9}$$

where

τ surface shear stress

ρ gas density

If the definitions for friction coefficient

$$f \equiv \frac{\tau}{\rho U^2} R^{1/6} \tag{10}$$

generalized momentum thickness

$$T \equiv \theta R^{1/6} \tag{11}$$

and diffusion coefficient

$$D_T \equiv \frac{T}{U}\frac{dU}{dx} \tag{12}$$

are substituted into the momentum equation as in reference 3, there results

$$\frac{dT}{dx} = \frac{7}{6}\left[f - D_T\left(H + \frac{13}{7}\right)\right] \tag{13}$$

In order to complete the solutions of this equation for arbitrary D_T, two more equations are required: one to determine values of f, and one to determine the development of the form factor H.

Region of constant velocity. - In the region of constant velocity $D_T = 0$, so that the momentum equation reduces to

$$\frac{dT}{dx} = \frac{7}{6} f \tag{14}$$

Falkner's data (reference 7) for surface shear with constant velocity show that

$$f = 0.006534 \tag{15}$$

Equation (14) may therefore be integrated to give

$$T - T_{tr} = \frac{7}{6} f(x - x_{tr}) \tag{16}$$

where the subscript tr indicates the value at transition.

Conditions for diffusion without separation. - The system of equations proposed by Garner (reference 3) was selected to describe the development of the turbulent boundary layer because of its simplicity. In selecting a law for friction, Garner examines data for $R > 1250$ and shows that f is constant with a value of 0.006534 if $-0.01 < D_T < 0.004$. (This is Falkner's value of f for $D_T = 0$, reference 7). For $D_T < -0.01$ no correlation is obtained. In consideration of the lack of correlated data for high diffusion rates, $D_T \geq -0.01$ was selected for the range of diffusion rate and therefore $f = 0.006534$ is used for the friction coefficient.

The development of the form factor H required for solution of the momentum equation is described by an empirical equation developed by Garner in reference 3. The relation is

$$T \frac{dH}{dx} = -e^{5(H - 1.4)} \left[D_T + A (H - 1.4) \right] \qquad (17)$$

where $A = 0.0135$.

The problem is then to define a velocity distribution that will avoid separation of the turbulent boundary layer. Experience shows that when H reaches a value of about 2.0, with conventional velocity distributions it subsequently rises rapidly and separation occurs. Values of H for separation are therefore usually given in the range $2.0 < H < 2.6$. It is therefore proposed that one possible criterion for prescribing the velocity is that H rise to some value and thereafter remain constant and less than 2.6.

Equation (17) describing the development of H shows that if, $H < 1.4 + (-D_T/A)$, then $dH/dx > 0$ and H tends toward $1.4 + (-D_T/A)$. If $H > 1.4 + (-D_T/A)$, then equation (17) shows that $dH/dx < 0$ and therefore H always tends toward the value $1.4 + (-D_T/A)$.

If constant values of D_T are considered as possible conditions for determining the velocity distribution, then the momentum equation shows that for a given velocity change D_T should be as large a negative number as possible in order to reduce the surface for skin friction. (The rapid diffusion results in airfoils with relatively longer regions of constant maximum velocity and therefore larger airfoil circulations.) For reliability of the boundary-layer equations, it is desirable to maintain $D_T \geq -0.01$. Therefore a possible condition is $D_T = -0.01$, the largest rate of diffusion with $f = 0.006534$. The limiting value of H for this case is 2.14, a value that is probably, but not certainly, safe. Two values were therefore used in the velocity computations: $D_T = -0.01$, and $D_T = -0.006$, which corresponds to a limiting value of $H = 1.844$.

A third condition for prescribing the diffusion rate was also employed. According to reference 4, separation will result if

$$D_S \equiv \frac{\theta}{U} \frac{dU}{dx} R^{-0.08} = \frac{T}{U} \frac{dU}{dx} R^{-0.247} = D_T R^{-0.247} \qquad (18)$$

attains the value of -0.0013. The third type of velocity distribution computed was for the maximum diffusion rate with both $D_T \geq -0.01$ and $D_S \geq -0.00115$, a value arbitrarily assigned with the condition that it be greater than the separation value -0.0013.

Velocity distributions in the region of diffusion. - For the cases where D_T is constant, equations (12) and (17) are used to eliminate the differential of x, and to obtain

$$\frac{dU}{U} = -\frac{D_T}{A} e^{-5(H - 1.4)} \frac{dH}{H - 1.4 + D_T/A} \tag{19}$$

which integrates to

$$\log \frac{U}{U_0} = -\frac{D_T}{A} e^{5D_T/A} \left[Ei(-5H-5D_T/A + 7) - Ei(-5D_T/A) \right] \tag{20}$$

where

$$Ei(y) \equiv \int_{-\infty}^{y} \frac{e^k}{k} dk$$

is the exponential integral function (tabulated in reference 8), having the principal part of the integral for $y > 0$ (that is, for $H < 1.4 - D_T/A$). The constant of integration for $U = U_0$ was chosen at $H = H_0 = 1.4$. This value of H, U_0, and T_0 will not be included on any point of the airfoil if laminar diffusion precedes turbulent diffusion.

Equations (12) and (13) give

$$\frac{dT}{T} = \frac{7}{6}\left[\frac{f}{D_T} - \left(\frac{13}{7} + 1.4 - \frac{D_T}{A}\right)\right]\frac{dU}{U} - \frac{7}{6}\left(H - 1.4 + \frac{D_T}{A}\right)\frac{dU}{U} \tag{21}$$

For the factor dU/U of the second term on the right side, a substitution is made from equation (19) to obtain an equation that may be integrated to

$$\log \left(\frac{T}{T_0}\right) = \frac{7}{6}\left[\frac{f}{D_T} - \left(\frac{13}{7} + 1.4 - \frac{D_T}{A}\right)\right] \log \frac{U}{U_0} + \frac{7}{30}\frac{D_T}{A}\left[1 - e^{-5(H - 1.4)}\right] \tag{22}$$

The arc length is then given by

$$\frac{x-x_0}{T_0} = \int_{x_0}^{x} \frac{dx}{T_0} = \frac{1}{D_T} \int_{U_0}^{U} \frac{T}{T_0} \frac{dU}{U} \tag{23}$$

The curves for the boundary-layer parameters in the turbulent-diffusion region are shown in figure 4 for $D_T = -0.010$, $D_T = -0.006$, and maximum diffusion rate with $D_T \geq -0.01$ and $D_S \geq -0.00115$.

In solving the boundary-layer equations (13) and (17) (with $f = 0.006534$) with the condition $D_S \geq -0.00115$, the value of D_T rises with R. The limitation $D_T \geq -0.01$ was added at the high Reynolds numbers in order to keep D_T in the range for which the friction law $f = 0.006534$ is valid. The solution of the equations in the region of variable D_T was obtained by approximating each portion of the curve with the solution for D_T = constant = mean value of D_T in that step.

Relations between Velocity Distribution and Blade Reynolds Number

The relations between the velocity distribution and blade Reynolds number $U_f X/\nu$ are developed. Some of the results are given in graphical form, which permits the use of the generalized velocity-distribution curves developed for the laminar and turbulent boundary layers (figs. 2 and 4). These curves will give the velocity distribution in the region of diffusion if the scale constants L_l, U_0, and T_0 are known; the remainder of the surface is determined by the constant x_l or x_t.

As assistance in finding the appropriate constants, the quantity x_l/X (or x_t/X for completely turbulent diffusion) is plotted in figure 5 as a function of the Reynolds number $U_f X/\nu$ and the velocity ratio U_f/U_{max}. (The method of computing fig. 5 is presented in appendix B.) The curves should be applied in the following manner:

The Reynolds number $U_f X/\nu$ and velocity ratio U_f/U_{max} are selected. Examination of figure 5 will indicate whether the

diffusion is laminar, mixed, or turbulent. If the diffusion is laminar, figure 5 gives the value of x_l, and then $L_l = 0.441\, x_l$, which establishes the scale for the use of figure 2.

If the diffusion is altogether turbulent, figure 5 determines x_t and then

$$T_0 = X \frac{\left(1 - \frac{x_t}{X}\right)}{\left(\frac{X - x_0}{T_0}\right)} \tag{24}$$

where $(X - x_0)/T_0$ is given in figure 4 as a function of U_f/U_0 and $U_0 = U_{max}$.

The case of mixed diffusion is considered to be of no technical significance in this application because of uncertainty in locating the position of transition. The effect of Reynolds number is therefore considered only in regions of purely laminar or purely turbulent diffusion, although x_l/X and $\Phi/U_f X$ were computed for $R_{tr} = 250$ and $D_T = -0.01$ in the mixed-diffusion region.

Suction-surface potential. - A further step in computing airfoil performance is the integration of the velocity curves to obtain

$$\frac{\Phi}{U_f X} = \int_0^1 \frac{U}{U_f}\, d\left(\frac{x}{X}\right) \tag{25}$$

a dimensionless form of the potential on the suction surface. Results of the computations are shown in figure 6. The comparative magnitudes of the potentials for various values of D_T (or D_S), U_f/U_{max}, and the Reynolds number are significant because in the system used for estimating blade circulation, an increase in suction-surface potential is generally accompanied by an increase in blade circulation.

The obtainable potential is highest with the greatest diffusion rate (compare figs. 6(a) and 6(b)) because the maximum velocity is maintained along the largest portion of the airfoil surface. The most pronounced effect of Reynolds number is the increase in potential shown in the change from laminar diffusion to turbulent

diffusion (fig. 6(a)). The increase in potential begins at a Reynolds number in the vicinity of 80,000 to 90,000 and for $U_f/U_{max} > 0.6$ is fully realized at the blade Reynolds number approximately 260,000 for $D_S \geq -0.00115$ and $D_T = -0.006$ and approximately 180,000 for $D_T = -0.010$. This change increases with decreasing diffusion-velocity ratio U_f/U_{max}. Although there is no effect of Reynolds number on suction-surface potential for diffusion with a completely laminar boundary layer, the effect of increase in Reynolds number for turbulent diffusion is a decrease of potential for constant values of D_T. An insignificant effect is shown, however, when the criterion of Kalikhman for separation is applied (fig. 6(c)). Because at large Reynolds numbers the conditions $D_S = -0.00115$ is replaced by $D_T = -0.01$, the curves so constructed approach the curves for $D_T = -0.010$ in that region. (The large Reynolds number condition is equivalent to the assumption that the extent of the laminar boundary layer approaches zero.)

The case of infinite Reynolds number is of particular significance because it is the most conservative design with turbulent boundary layer for constant diffusion coefficient D_T. The potential at large Reynolds numbers was therefore computed and is shown in figure 7 for values of $D_T = -0.010$ and -0.006. The curve for $D_T = -0.010$ at high Reynolds numbers is practically the same as that of $D_S \geq -0.00115$ for all Reynolds numbers because the potential for the D_S-condition shows so little variation with Reynolds numbers.

The trend of curves shows that highest potential occurs at a U_f/U_{max} of approximately 0.58 with very little variation between 0.53 and 0.63. Therefore, if a design is considered with a preassigned value for the velocity diagram and U_f, there is negligible gain in using higher peak velocities than $U_{max} \approx 1.6\ U_f$. For diffusion with a laminar boundary layer, figure 3 shows negligible increase in obtainable potential for peak velocities U_{max} higher than $1.25\ U_f$.

Deviations from design conditions. - A knowledge of the range of operation of any cascade of airfoils is essential in determining its suitability for application. For the sets of blades considered here, the effect of change of Reynolds number is nonexistent with purely laminar diffusion. A very slight and indeterminate effect is shown for turbulent diffusion with $D_S \geq -0.00115$. If the limitations imposed by constant D_T are closer to the physical facts, then less lift is obtainable at higher Reynolds numbers.

Consequently, increase in Reynolds number of operation would involve the danger of separation. A safe estimate of lift would therefore be made on the basis of the potential for the maximum Reynolds number of operation provided the minimum Reynolds number of operation does not extend into the regions requiring laminar diffusion rates. If the maximum Reynolds number of operation is taken to be three times the minimum, then a very slight effect of design Reynolds number on potential is indicated even for the diffusion rates $D_T = -0.010$ and -0.006. The Reynolds numbers at which some diffusion with laminar boundary layer occurs depend on the value selected for R_{tr} (in this case 250), on the diffusion rate, and on the velocity ratio U_{max}/U_f. Estimates of lift made on the basis of $D_T = -0.010$ and $RN \rightarrow \infty$ would be in agreement with estimates based on $D_S \geq -0.00115$. If a blade designed on such a basis was used at low enough Reynolds numbers, then the laminar boundary layer existing in the region of diffusion would separate because of too steep a pressure gradient.

If a rough finish or a higher angle of attack than the design value occur in application of the blade, an increase in the value of T_t over the design value may be expected. Then the initial value of $D_T = T\left(\frac{1}{U}\frac{dU}{dx}\right)$ will increase in the same proportion at the beginning of diffusion. Sample computations show, however, that for velocity distributions based on constant D_T, this initial increased value for D_T is not maintained but drops to some value intermediate between the initial value and the value for which the velocity distribution was prescribed. If the value of the form factor for separation H is assumed to be 2.2, it would correspond to the limit for a constant value of D_T given by

$$D_T = -0.0135\ (H - 1.4) = -0.0108$$

If the design velocity distribution corresponded to $D_T = -0.006$ (limiting $H = 1.85$), and then in operation T were increased by 80 percent to give an initial value of $D_T = -0.0108$, the resulting limiting value of D_T would be greater than -0.0108 (less in absolute value) and the limiting value of H would be less than 2.2; thus, according to this criterion, separation would be avoided. If the design velocity distribution corresponded to $D_T = -0.010$, however, an increase of 80 percent of T would result in separation according to this criterion.

ESTIMATE OF BLADE CIRCULATION AND SPACING

Effect of Thickness

An approximate calculation is made for the blade circulation from the upper-surface velocity distribution by a modification of the method for thin airfoils. The basic idea is that the airfoil-surface velocity is the sum of two components, one of which results from the basic thickness form uncambered, and the second of which results from the curvature of the camber line. The suction-surface velocity of the thin, slightly cambered, isolated airfoil is then given by

$$U' = \overline{U}' + \Delta U' = V' \left(\frac{\overline{U}'}{V'} + \frac{\Delta U'}{V'} \right)$$

where

U' suction-surface velocity of airfoil

$\overline{U}'$ velocity component resulting from uncambered thickness distribution

$\Delta U'$ velocity increment resulting from curvature of camber line

V' free-stream velocity

The ratios $\overline{U}'/V'$ and $\Delta U'/V'$ are independent of the magnitude of V'. A similar equation holds for the pressure surface,

$$U_p' = \overline{U}' - \Delta U' = 2\overline{U}' - U'$$

where U_p' is the velocity on the pressure surface. If the suction-surface velocity is known, and if the velocity component $\overline{U}'$ resulting from the thickness can be determined, then the pressure-surface velocity can be computed.

In applying these ideas to the cascade, the principal change is the use of the distorted flow field in which the airfoil is immersed; the quantity V' is now regarded as a variable quantity. Near the leading edge, the velocity V_1 is substituted for V' giving

$$\overline{U}_i = V_1 \left(\frac{\overline{U}_i'}{V'} \right) \tag{26}$$

where the subscript i indicates the value near the leading edge, and $\bar{U}_i'/V'$ is the velocity rise over the free-stream value for the isolated airfoil. The value for $\bar{U}'/V'$ is a function of the assumed thickness distribution. Similarly, near the trailing edge the free-stream value used is V_2 giving

$$\bar{U}_f = V_2 \left(\frac{\bar{U}_f'}{V'}\right) \tag{27}$$

At the point of the airfoil where the air has been turned halfway so that the flow direction is given by the angle α_m where

$$\tan \alpha_m = \frac{1}{2} (\tan \alpha_1 + \tan \alpha_2) \tag{28}$$

where

α angle between velocity vector and normal to cascade axis

Subscripts:

1 value for upstream of cascade

2 value for downstream of cascade

the same procedure might be used as for the leading and trailing sections of the airfoil with the substitution of V_m for V' in the equation for $\bar{U}_m$. The value of V_m is computed from the continuity equation

$$V_1 \cos \alpha_1 = V_2 \cos \alpha_2 = V_m \cos \alpha_m \tag{29}$$

which does not include the effect of airfoil thickness in blocking the flow area and increasing the flow velocity. If the spacing s is not too small, the correction for the distorted flow that is applied is

$$V_{m,c} = \frac{V_m}{1 - \frac{\pi^2}{48}\left(\frac{X}{s}\right)^2 \left(\frac{\bar{U}'}{V'} - 1\right) \cos 2\alpha_m}$$

This formula is derived in appendix C. Then,

$$\bar{U}_m = V_{m,c}\left(\frac{\bar{U}'}{V'}\right) = V_m\left[\frac{\bar{U}'/V'}{1 - \frac{\pi^2}{48}\left(\frac{X}{s}\right)^2\left(\frac{\bar{U}'}{V'} - 1\right)\cos 2\alpha_m}\right] \tag{30}$$

When the blade spacing is very small, however, it becomes more accurate to regard the flow between the blades as flow in a channel. From this standpoint, the flow velocity is increased over V_m by the ratio of the flow area without blade thickness to the flow area with blade thickness. That is, the effect of thickness is given by

$$\bar{U}_m = V_m\left(\frac{s}{s - t_m \sec \alpha_m}\right) \tag{31}$$

where t_m is the blade thickness at the point x_m where the air flow has been turned to the direction α_m. This equation is applied only if the point of application of the lift force x_m is within a range of values specified by

$$\frac{s}{2} < x_m < X - \frac{s}{2} \tag{32}$$

This condition was selected because it is believed that inside this range the effect of variations of inflow and outflow direction on the velocity is expected to be small enough to be neglected for the purpose of the calculation. Thus, the flow is expected to be essentially that inside a long channel.

Relations have been developed for computing $\bar{U}$ at three points on the airfoil. The family of airfoil cascades being considered will be restricted by assuming a second-degree parabola connecting the points $(0, \bar{U}_i)$, $(x_m, \bar{U}_m)$, and $(X, \bar{U}_f)$. That is,

$$\frac{\bar{U}}{U_f} = \frac{\bar{U}_i}{U_f} + B^{(1)}\frac{x}{X} + B^{(2)}\left(\frac{x}{X}\right)^2 \tag{33}$$

where

$$\left.\begin{aligned} B^{(1)} &= \frac{\bar{U}_f}{U_f} - B^{(2)} - \frac{\bar{U}_i}{U_f} \\ B^{(2)} &= \frac{\bar{U}_i/U_f}{x_m/X} - \frac{\bar{U}_m/U_f}{(x_m/X)(1 - x_m/X)} + \frac{\bar{U}_f/U_f}{(1 - x_m/X)} \end{aligned}\right\} \tag{34}$$

Estimate of Circulation and Spacing

By assuming that $\bar{U}_i$, $\bar{U}_m$, and $\bar{U}_f$ are known, the curve for $\bar{U}$ can then be determined when the value of x_m is found. Because x_m is the center of pressure, it may be found as the weighted mean value of x; the weight assigned to each value is the local blade loading.

Because x_m is at the center of pressure,

$$x_m = \frac{\int_0^{\Gamma} x \, d(\varphi - \varphi_p)}{\Gamma} \tag{35}$$

where

φ potential on upper surface measured from leading edge to a point x

Γ airfoil circulation, $(\Phi - \Phi_p)$

Φ value of φ at trailing edge

The quantity,

$$\Phi = \int_0^{X} U \, dx = U_f X \left(\frac{\Phi}{U_f X}\right)$$

may be found from either figures 3, 6, or 7. The quantity,

$$\int_0^{\Phi} x d\varphi = \int_0^{X} xU \, dx \equiv U_f X^2 \, m$$

may be found from figure 8. The curves for $D_T = -0.010$ are approximately correct for $D_S \geq -0.00115$.

For calculation of the potential φ_p, the high camber of airfoils in cascade must be considered because it results in a substantially different length of the suction and pressure

surfaces unlike isolated airfoils, which are nearly straight. The effect of the difference in length is approximated by setting

$$x_p = \beta x \tag{36}$$

where β is some constant nearly equal to unity. The circulation is thus,

$$\Gamma = \int_0^X U\,dx - \int_0^{X_p} U_p\,dx_p = \int_0^X \left[U - \beta\,(2\bar{U} - U)\right] dx$$

$$\Gamma = \Phi - \left[2\beta \int_0^X \bar{U}\,dx - \beta\Phi\right] = \Phi - \Phi_p \tag{37}$$

where

$$\Phi_p = 2\beta \int_0^X \bar{U}\,dx - \beta\Phi \tag{37a}$$

Using equation (33) for $\bar{U}$, there are obtained,

$$\int_0^X \bar{U}\,dx = U_f X \left[\frac{1}{2}\left(\frac{\bar{U}_f}{U_f} + \frac{\bar{U}_i}{U_f}\right) - \frac{B^{(2)}}{6}\right] \tag{38}$$

and

$$\int_0^{\Phi_p} x\,d\varphi_p = \beta \int_0^X x\,U_p\,dx = \beta \int_0^X x\,(2\bar{U} - U)\,dx$$

with

$$\int_0^X \bar{U}\,x\,dx = U_f X^2 \left(\frac{1}{2}\frac{\bar{U}_i}{U_f} + \frac{B^{(1)}}{3} + \frac{B^{(2)}}{4}\right) \tag{39}$$

The factor β is estimated on the assumption that the airfoil suction surface and pressure surface are circular arcs intersecting at the leading and trailing edges. The angle of turning $\bar{\lambda}$ of the mean line is assumed equal to the air deflection:

$$\bar{\lambda} = \alpha_1 - \alpha_2$$

The turning λ of the suction surface is then computed from

$$\sin \frac{\lambda - \bar{\lambda}}{4} = \frac{t}{X} \frac{\lambda \cos \bar{\lambda}/4}{4 \sin (\lambda/4)} \tag{40a}$$

Then the turning of the pressure surface λ_p is computed from

$$\tan \frac{\lambda_p}{4} = \tan \frac{\lambda}{4} - 2 \frac{t}{X} \frac{\lambda}{2 \sin \frac{\lambda}{2}} \tag{40b}$$

The ratio of lengths is

$$\beta \equiv \frac{X_p}{X} = \frac{\lambda_p}{\lambda} \frac{\sin \lambda/2}{\sin \lambda_p/2} \tag{41}$$

Substituting the values for the integrals (38) and (39) in equation (35), there results

$$C^{(3)} \left(\frac{x_m}{X}\right)^3 + C^{(2)} \left(\frac{x_m}{X}\right)^2 + C^{(1)} \left(\frac{x_m}{X}\right) + \frac{\bar{U}_m - \bar{U}_i}{12 U_f} = 0 \tag{42}$$

where

$$\left.\begin{aligned} C^{(3)} &\equiv \frac{\bar{U}_i + \bar{U}_f}{2 U_f} - \left(\frac{1 + \beta}{2 \beta}\right) \frac{\Phi}{U_f X} \\ C^{(2)} &\equiv \left(\frac{1 + \beta}{2\beta}\right) \frac{\Phi}{U_f X} + \left(\frac{1 + \beta}{2\beta}\right) m - \frac{2}{3} \frac{\bar{U}_f}{U_f} - \frac{5}{6} \frac{\bar{U}_i}{U_f} \\ C^{(1)} &\equiv \frac{5}{12} \frac{\bar{U}_i}{U_f} + \frac{1}{4} \frac{\bar{U}_f}{U_f} - \frac{1 + \beta}{2\beta} m - \frac{1}{6} \frac{\bar{U}_m}{U_f} \end{aligned}\right\} \tag{43}$$

With the values for $\bar{U}_i$, $\bar{U}_m$, and $\bar{U}_f$ equation (42) may be solved for x_m, equation (34) for $B^{(1)}$ and $B^{(2)}$, and finally the curve for $\bar{U}$ (equation (33)) determined. Furthermore, equations (37a) and (38) determine the potential Φ_p, so that the dimensionless circulation $\Gamma/U_f X$ is then

$$\frac{\Gamma}{U_f X} = \frac{\Phi}{U_f X} - \frac{\Phi_p}{U_f X} \tag{44}$$

For potential flow,

$$\Gamma = s\,(V_1 \sin \alpha_1 - V_2 \sin \alpha_2)$$

The velocity V_1 may be eliminated by the continuity equation (24) resulting in

$$\frac{X}{s} = \frac{V_2}{U_f} \frac{\cos \alpha_2\,(\tan \alpha_1 - \tan \alpha_2)}{\frac{\Gamma}{U_f X}} \tag{45}$$

which determines the blade spacing.

Comparison with Exact Procedure

For the purpose of judging the accuracy of the method of estimating the pressure-surface-velocity distribution, a comparison was made with velocities computed for potential flow by an exact procedure. The data were obtained from reference 9. The comparison is shown in figures 9(a) and 9(b). In both cases, values of $\bar{U}'/V'$ were selected to fit approximately the NACA 65-series isolated airfoil data (reference 10), which gave

$$\left.\begin{aligned} \frac{\bar{U}_i'}{V'} &= 1.025 \\ \frac{\bar{U}_m'}{V'} &= 1 + 1.35\,\frac{t_m}{X} \\ \frac{\bar{U}_f'}{V'} &= 0.950 \end{aligned}\right\} \tag{46}$$

By using these values and equations (26), (27), (29), and (30), $\bar{U}_i/V_m$, $\bar{U}_f/V_m$, and $\bar{U}_m/V_m$ were computed. Next β was obtained by use of equations (40) and (41). Evaluation of the data for suction-surface-velocity distribution yielded Φ/V_mX and $m(U_f/V_m)$. It was now possible to substitute all these values into equations (43) and solve for x_m/X by use of equation (42). The solution was then continued in the manner indicated in the previous section.

Pressure-surface velocity was then plotted using the equation

$$\bar{U} = \frac{U + U_p}{2}$$

The shapes of the estimated and exact velocity distribution on the pressure surface are quite similar. The solidity computed from the estimated velocities is, however, 6-percent higher for figure 9(a) and 4-percent lower for figure 9(b) than the exact value. These values then give an indication of the order of inaccuracy of the method of estimating solidity. The error in pressure-surface potential Φ_p was 6 percent for the airfoil of figure 9(a) and 2 percent for the airfoil of figure 9(b).

EFFECT OF SEVERAL PARAMETERS ON REQUIRED CASCADE SOLIDITY

The relations developed in the previous section are applied to study the effect of several design and operating parameters on required cascade solidity.

Computations

The data given in the problems solved consisted of the following: (1) Reynolds number U_fX/ν (either very high or very low); (2) diffusion coefficient D_f (either -0.010 or -0.006 for a turbulent boundary layer); (3) trailing-edge loading $(U_f-\bar{U}_f)/V_2$ (assumed to be 0.1 because cascade data indicated this value as attainable); (4) velocity ratio U_{max}/V_2; (5) velocity-diagram components V_1, V_2, α_1, and α_2 from which V_m and α_m are computed; and (6) velocity ratios $\bar{U}_i'/V'$, $\bar{U}_m'/V'$, and $\bar{U}_f'/V'$, which are determined from the assumed basic thickness distribution. In all cases the assumed values were $\bar{U}_i'/V' = 1.025$ and

$\bar{U}_f/V' = 0.95$, but $\bar{U}_m'/V'$ was varied to obtain various values for the thickness. All the assumed quantities were varied in the examples to show the effect on the required cascade solidity, the velocity distribution, and the thickness. The sequence of computation is:

(1) Compute

$$\frac{\bar{U}_i}{V_1} = \frac{\bar{U}_i'}{V'} = 1.025$$

$$\frac{\bar{U}_f}{V_2} = \frac{\bar{U}_f'}{V'} = 0.95$$

$$\frac{U_f}{V_2} = \frac{\bar{U}_f}{V_2} + \left(\frac{U_f - \bar{U}_f}{V_2}\right) = 1.05$$

$$\frac{U_f}{U_{max}} = \frac{\left(\frac{U_f}{V_2}\right)}{\frac{U_{max}}{V_2}}$$

(2) From U_f/U_{max}, the assumption of either laminar or turbulent diffusion, and the desired rate of diffusion, figures 2 to 8 are used to find the suction-surface-velocity distribution and the values for Φ/U_fX and m.

(3) Values for the solidity X/s and the pressure center x_m/X are assumed. The thickness is then computed from equations (30) and (46) if either $x_m/s < 0.5$ or $x_m/s > X/s - 0.5$. If $0.5 < x_m/s < X/s - 0.5$, then equation (31) is used. The factor β is then obtained from equations (40) and (41).

(4) The quantities $C^{(3)}$, $C^{(2)}$, $C^{(1)}$, x_m, $B^{(1)}$, $B^{(2)}$, Φ/U_fX, Γ/U_fX, and X/s are next computed from equations (43), (42), (34), (38), (44), and (45).

(5) Steps (3) and (4) must be repeated if the solidity X/s varies considerably from the assumed value or if, because of an incorrect assumption for x_m, an incorrect choice was made in the equation for the computation of t_m/X and β.

Results

The results of the computations are shown in the following table and in figure 10. The table gives the assumed values for the design parameters and the computed solidity, whereas figure 10 shows the details of the velocity distributions with sketches to indicate the cascade solidity and the airfoil thickness. The circles drawn on the camber lines indicate the location of x_m and the airfoil thickness t_m.

Case	Boundary layer	Diffusion coefficient	α_1 (deg)	α_2 (deg)	$\frac{U_{max}}{V_2}$	$\frac{U_f-\bar{U}_f}{V_2}$	$\frac{t_m}{X}$	$\frac{X}{s}$
a	Turbulent	-0.010	45	38	1.615	0.10	0.10	0.30
b	Turbulent	- .010	45	38	1.312	.10	.10	.64
c	Turbulent	- .010	45	38	1.312	.10	.06	.50
d	Turbulent	- .010	45	38	1.312	.00	.06	.65
e	Turbulent	- .010	45	-45	1.615	.10	.20	1.6
f	Turbulent	- .010	45	-45	1.615	.10	.15	1.3
g	Turbulent	- .010	45	-45	1.312	.10	.11	1.8
h	Turbulent	- .010	0	-45	1.312	.10	.18	1.0
i	Turbulent	- .006	45	38	1.615	.10	.10	.42
j	Turbulent	- .006	45	38	1.312	.10	.06	.56
k	Laminar	- .06618	45	38	1.615	.10	.06	1.6
l	Laminar	- .06618	45	-45	1.312	.10	.08	3.1
m	Laminar	- .06618	0	-45	1.312	.10	.09	1.7

The effect of variation of maximum surface velocity U_{max} on solidity X/s of a compressor-type blade is shown by comparison of cases (a) and (b) where all design parameters are the same except U_{max}/V_2. The blade with a lower value of U_{max}/V_2 is obviously better suited for operation with a compressible fluid with a high Mach number, but has the disadvantage of requiring a higher solidity (twice as many blades).

If in case (b) the thickness is reduced from 0.10 to 0.06, the cascade corresponding to case (c) results, having only 78 percent of the solidity of case (b). This decrease results from the higher aerodynamic loading of the thinner blade because of the lower pressure-surface velocities caused by the thickness.

In cases (a), (b), and (c), the trailing-edge loading corresponds to an air flow that does not satisfy the Kutta condition. The actual blade having the prescribed velocity distribution would have an extension from the point $x/X = 1.0$ to larger values in

which the loading would drop to zero. Similarly, the initial parts of the velocity distributions do not include the leading edge. That is, the velocity distributions shown do not extend over the entire airfoil, but do include practically all the aerodynamically loaded region. A velocity distribution was computed for zero trailing-edge loading (case (d)) in order to observe what sacrifice would be involved in avoiding separation at the trailing edge and attempting an airfoil design that would satisfy the Kutta condition. Comparison with case (c) shows that the solidity is about 1.3 times as great. The effect would be less in the case of reaction blading where the inlet velocity results in large loading in the initial part of the airfoil and a relatively smaller effect of trailing-edge loading. The effect of decrease in trailing-edge loading is also less for blades of small diffusion ratio U_{max}/U_f, because in such cases the suction-surface velocity is maintained at its maximum value to a point very close to the trailing edge and, as a consequence, the loading is also maintained over most of the airfoil.

For an impulse blade $(V_2 = V_1)$ of large turning (turbine type), the velocity distribution is very much the same as for a compressor blade with nearly the same velocity curves $\overline{U}$ and U, although the thickness will radically vary because of the low value for V_m. For example, compare cases (a) and (e).

If the turbine-blade thickness is reduced to the value closer to the compressor blade, the circulation is increased (case (f)), as might be expected. The large diffusion ratio on the pressure surface, which practically insures the existence of a separation bubble there, should also be noted.

The effect of decreasing the maximum surface velocity U_m is shown in case (g), which has lower blade circulation even though the thickness was decreased from 0.15 to 0.11. Solidity increased 39 percent over the value for case (f).

For an inlet guide vane turning the air from an angle of 0° to an angle of -45° (case (h)), the velocity distribution changes from the impulse cascade (case (g)) because of the large decrease in the inlet velocity. Even with the increased thickness, local velocities on the pressure surface do not involve high diffusion rates because of the over-all increase in velocity $(V_1/V_2 = 0.707)$.

The effect of reducing the rate of diffusion from that of cases (a) and (c) $(D_T = -0.010)$ to a lower rate $(D_T = -0.006)$, while maintaining the same values of the other design parameters, was

determined by computing the corresponding cases (i) and (j), respectively. The positions at which the $\bar{U}/V_2$ values are equal for the two cases are where the values of α are the same. There is some chordwise shift in the location of a given value of α when changing from case (a) to case (i) because of the shift in the loading distribution. Consequently, the location of x_m shifts and the thickness distribution changes. The last half of the blade (case (i)) does very little turning so that the solidity increases from 0.31 to 0.42. The usefulness of this part of the blade could be greatly increased if a larger turning of the air were involved, for the $\bar{U}/V_2$ curve would rise to higher values in the first half of the airfoil and drop to lower values in the last half, thus shifting the load backwards on the blade surface. The change in velocity and solidity from case (c) to case (j) is slight because the rate of diffusion has very little effect on suction-surface potential when the diffusion is small. (See fig. 7.)

An effect of blade Reynolds number U_1X/ν is shown by comparison of cases (a) and (k). In case (k), the expansion is entirely laminar (low Reynolds number), whereas in case (a) the extent of the laminar region is assumed zero (high Reynolds number). Even though the laminar-layer blade is only 6-percent thick, the solidity (1.6) required is five times as large as for the blade with a turbulent boundary layer. This loss in circulation results from the fact that laminar diffusion must be begun so much earlier when the boundary layer is thinner. On the pressure surface of the blade is to be observed a region near the trailing edge where the rate of diffusion increases to a value that will certainly induce separation. A better aerodynamic design could be obtained with a thinner blade, which would be necessary if the turning were greater. Some improvement would also probably result with a less simple mean velocity curve. It appears safe to conclude that it is extremely difficult, if not impossible, to obtain a compressor blade of reasonable thickness and turning, if flow separation is to be avoided with a laminar boundary layer.

The design of an impulse blade with laminar boundary layer appears to be entirely feasible (case (l)) as a consequence of the low value for $\bar{U}_m/V_2$, which is a result of the low value for V_m/V_2. A reaction blade with laminar boundary layer also is feasible. (See case (m).) The percentage increase in solidity for cases (l) and (m) over that for cases (g) and (h) is much less than the percentage increase in solidity for case (k) over that for case (a). As a general rule, cascade solidities for laminar and

turbulent diffusion can be expected to be more nearly alike when diffusion is small ($U_{max}/U_f \rightarrow 1.0$) than when diffusion is large ($U_{max}/U_f \rightarrow 2.0$), because of the smaller difference in suction-surface potential. (See fig. 6(a).)

COMPARISON OF EXPERIMENTAL WITH INDICATED ATTAINABLE SOLIDITY VALUES

In order to estimate the degree with which blades in use approach the maximum attainable circulation as indicated by the present method of analysis, cascade solidities were computed for conditions comparable to those for which performance data were available. It was desired to compare the solidities of the tested blades and those corresponding to the proposed velocity distributions on the basis of operation at very low Mach numbers, very high Reynolds number, the same values for α_1, α_2, maximum thickness t/X, U_{max}/V_2, and U_f/V_2. The data available did not give all this information, or did so with no indication as to the efficiency of the cascade. Data used were obtained from references 11 and 12. In none of the comparisons shown is it possible to evaluate cascade efficiency, although for every case the comparison was made on the basis of the optimum operating condition of the cascade as stated. The comparisons are shown in the following table:

Reference	Blade designation	α_1 (deg)	α_2 (deg)	U_{max}/V_2	Experimental X/s	Estimated X/s	
						$D_T = -0.010$	$D_T = -0.006$
11	65-(18)10	45	15	1.699	1.063	1.68[a]	----------
11	65-(12)10	45	23.8	1.602	1.034	1.17	1.60
11	65-(4)10	45	37.0	1.300	1.013	.78	.88
11	65-(0)10	45	42.9	1.186	1.003	.36	.38
12	64-(A)06	0	-45.8	1.180	1.538	1.12	----------
12	64-(B)06	0	-52.0	1.133	1.534	1.20	----------

[a] $t/X = 0.0664$.

All of the cases are directly comparable as previously described except the 65-(18)10 blade, for which it was impossible to find a solution with 10-percent thickness, indicating a strong probability of separated flow on the blade. A solidity was computed with the thickness reduced to 6.64 percent.

The 65-(12)10 blade has a lower solidity and therefore a higher circulation than either of the estimates for a maximum-circulation blade. Possible causes for this discrepancy are: (1) slight flow separation from the surface of the 65-(12)10 blade, and (2) the assumption of a parabolic curve for $\bar{U}$, which may involve some sacrifice in attainable circulation. For lower diffusion (65-(4)10 and 65-(0)10) and for reaction blades (64-(A)06 and 64-(B)06), the estimates indicate that higher circulations are attainable. The 64-(A)06 and 64-(B)06 blades have such high values for U_f/U_{max} that there is no substantial difference when the lower diffusion rate $D_T = -0.006$ is used in the solidity estimate. It seems reasonable to expect that higher blade circulations are obtainable with blades other than the 65- and 64-series for low pressure rise and for pressure drop. The 65-(0)10 blade is particularly subject to improvement.

CONCLUSIONS

The analysis of the limitations on the circulation about blades in cascade indicates that under the assumption of the several criteria for separation and the avoidance of local separation of the flow, the following conclusions can be drawn:

1. For a preassigned maximum velocity and suction-surface trailing-edge velocity, the suction-surface potential and airfoil circulation increases with the increase in permissible diffusion rate.

2. For a laminar boundary layer, Loitsianskii's equation determines blade circulations independent of the Reynolds number. For a turbulent boundary layer, Kalikhman's criterion for safe diffusion ($D_S \geq -0.00115$) indicates very slight changes in blade circulation with variation in Reynolds number. If a constant diffusion rate ($D_T = -0.010$ or -0.006) is used, however, some slight decrease in attainable potential with increase in Reynolds number is indicated. There is a very marked increase in obtainable lifts when the design is changed from that for a laminar boundary layer to that for a turbulent boundary layer. This effect decreases with decrease in the diffusion ratio U_{max}/U_f or U_{max}/V_2. With transition at momentum-thickness Reynolds number R = 250, the change begins to occur at a blade Reynolds number RN between 80,000 and 90,000. For completely turbulent diffusion with $U_f/U_{max} > 0.6$, the blade Reynolds numbers are 260,000 (Kalikhman's criterion and $D_T = -0.006$) and 180,000 ($D_T = -0.010$).

3. Suction-surface potential and consequently the airfoil circulation increases with increasing maximum velocity ratio U_{max}/V_2 or

U_{max}/U_f; however, negligible gain in circulation is obtained with U_{max}/U_f greater than 1.6 with turbulent diffusion and greater than 1.25 with laminar diffusion.

4. An airfoil designed for laminar boundary layer may be operated at any Reynolds number. An airfoil designed for a turbulent boundary layer has a lower Reynolds number limit for operation without separation. This limit is a function of the velocity ratio U_{max}/U_f, the diffusion rate, and the condition for transition. For R = 250, and diffusion velocity ratios $U_{max}/U_f < 1.67$, the lower limit of RN is equal to or less than 260,000 for small diffusion rates ($D_T = -0.006$, $D_S \geq -0.00115$) and equal to or less than 180,000 for larger diffusion rates ($D_T = -0.010$).

5. Improvement in airfoil circulation always results from adding loading at the trailing edge, but the improvement is less with decrease in over-all diffusion (decrease in V_1/V_2) and with decrease in surface diffusion (decrease in U_{max}/U_f).

6. Change in suction-surface-velocity distribution resulting from change in diffusion coefficient or character of the boundary layer has a large effect on blade circulation except when the diffusion is small. This small effect is to be expected in blades designed for high-speed operation and for reaction blades.

7. For a fixed suction-surface-velocity distribution, obtainable blade circulation decreases with increasing blade thickness.

8. The large discrepancy between the circulation of the 65-(18)10 blade with the recommended velocity diagram and the estimated attainable circulation implies a strong possibility of separation of the flow from the 65-(18)10 blade. For the recommended conditions of operation of the 65-(4)10, 65-(0)10, 64-(A)06, and 64-(B)06 blades, estimates indicate that higher blade circulations are attainable.

Lewis Flight Propulsion Laboratory,
National Advisory Committee for Aeronautics,
Cleveland, Ohio, June 6, 1949.

APPENDIX A

SYMBOLS

The following symbols are used in this report:

A	0.0135
$B^{(1)},B^{(2)}$	coefficients of (x/X) and $(x/X)^2$ terms in equation for $\bar{U}$
$C^{(1)},C^{(2)},C^{(3)}$	coefficients of (x_m/X), $(x_m/X)^2$, and $(x_m/X)^3$ terms in equation for x_m
c	chord
D_L	diffusion coefficient with laminar boundary layer, $\left(\frac{L}{\bar{U}}\frac{dU}{dx}\right)$
D_S	$\left(\frac{\theta}{\bar{U}}\frac{dU}{dx}R^{-0.08}\right)$ (according to Kalikhman, separation occurs when $D_S = -0.0013$)
D_T	diffusion coefficient with turbulent boundary layer, $\left(\frac{T}{\bar{U}}\frac{dU}{dx}\right)$
$Ei(y)$	exponential integral, $\left(\int_{-\infty}^{y}\frac{e^k}{k}dk\right)$
F	parameter in approximate equations for laminar boundary layer
f	coefficient of friction, $\left(\frac{\tau}{\rho U^2}R^{1/6}\right)$
H	form factor, (δ^*/θ)
L	generalized momentum thickness of laminar boundary layer, (θR)
m	$\frac{1}{U_1X^2}\int_0^X xU\,dx$
R	momentum-thickness Reynolds number, $(U\theta/\nu)$

RN	blade Reynolds number, $(U_f X/\nu)$
s	spacing of airfoils along cascade axis
T	generalized momentum thickness of turbulent boundary layer, $(\theta R^{1/6})$
t	thickness of airfoil
U	suction-surface velocity just outside boundary layer
$\overline{U}$	arithmetic average of suction- and pressure-surface velocities
V	stream velocity
$V_{m,c}$	V_m corrected for thickness effect of airfoils in cascade
X	total suction-surface length
x	arc length on airfoil suction surface
α	angle between velocity vector and normal to cascade axis
β	ratio of pressure-surface length to suction-surface length, (x_p/x)
Γ	circulation around one airfoil
δ^*	displacement thickness of boundary layer
θ	momentum thickness of boundary layer
λ	turning angle of upper surface
$\overline{\lambda}$	turning angle of camber line
ν	kinematic viscosity of gas
ρ	gas density
τ	surface shear stress
Φ	complete velocity potential, $\left(\int_0^X U dx\right)$
φ	velocity potential, $\left(\int_0^x U dx\right)$ measured from leading edge

Subscripts:

f	final value near trailing edge
i	initial value near leading edge
l	value at beginning of laminar diffusion process
m	value corresponding to mean of upstream and downstream velocity vectors
max	maximum value
p	value on pressure surface
t	value at beginning of turbulent diffusion process
tr	value at transition
0	value corresponding to $H = 1.400$ in turbulent boundary layer
1	upstream value
2	downstream value

Superscript:

$'$	pertaining to isolated airfoil

APPENDIX B

METHOD OF COMPUTING FIGURE 5

For diffusion with a laminar boundary layer, equations (7a) and (8) determine for any given velocity ratio U_f/U the value for x_l. Then

$$L_l = 0.441\ x_l$$

For the case of diffusion with partly laminar and partly turbulent boundary layer, a number of values were selected for

$$R_l = \frac{\theta_l\ U_l}{\nu}$$

the Reynolds number at the beginning of laminar diffusion. The units of velocity and length may be taken as U_l and x_l, respectively. Also

$$L_l = 0.441\ x_l$$

which establishes the scale of the laminar-diffusion region. At the transition point, $R_{tr} = \frac{\theta_{tr}\ U_{tr}}{\nu} = 250$, so that for L_{tr} there is obtained from equation (6d)

$$L_{tr} = L_l \left(\frac{R_{tr}}{R_l}\right)^{\frac{2(F+D_L)}{F\ +\ 2D_L}}$$

and

$$\frac{U_{tr}}{U_l} = \frac{U_{tr}}{U_{max}} = \left(\frac{R_{tr}}{R_l}\right)^{\frac{2D_L}{F\ +\ 2D_L}}$$

Because,

$$L = \theta R$$

then

$$\theta_{tr} = \frac{L_{tr}}{R_{tr}}$$

and

$$T_{tr} = \theta_{tr} (R_{tr})^{1/6}$$

The initial condition for H is

$$H_{tr} = 1.4 - \frac{D_{T,tr}}{0.0135}$$

(reference 3), where

$$D_{T,tr} \equiv \left(\frac{T}{U}\frac{dU}{dx}\right)_{tr} = D_L(R_{tr})^{5/6}$$

For this value of H_{tr}, figure 4 identifies U_{tr}/U_0 and R_{tr}/R_0, thus establishing the scale for the velocity U and the basic length T_0. By proceeding to the final velocity U_f, the length $X - x_{tr}$ is established, and $RN = U_f X/\nu$ may be computed.

If the diffusion is entirely turbulent, then by assuming a value for the Reynolds number at the beginning of turbulent diffusion R_t, there are obtained (x_{tr} and U_{tr} are taken as the units of length and velocity, respectively)

$$\theta_{tr} = 0.441 \frac{x_{tr}}{R_{tr}}$$

$$T_{tr} = \frac{0.441\ x_{tr}}{(R_{tr})^{5/6}}$$

$$D_{T,tr} = 0$$

$$H_{tr} = 1.4$$

$$U_0 = U_{max}$$

$$T_0 = T_{tr}$$

APPENDIX C

EFFECT OF AIRFOIL THICKNESS ON FLOW THROUGH CASCADES

By assuming that the effect of the airfoil circulation on the velocity at the point x_m (where the flow has turned to the direction α_m) is taken into account by the turning effect, the change in velocity from V_1 to V_m is given by

$$V_m = V_1 \cos \alpha_1 \sec \alpha_m$$

The effect of thickness is now separately evaluated as the approximate effect of a cascade of uncambered airfoils of stagger α_m with no circulation. The thickness distribution is assumed similar to that of a Joukowsky airfoil, which is discussed generally in reference 13. The potential function W for a uniform stream of velocity V flowing about a Joukowsky airfoil of small thickness can be shown to be

$$W = V\left[\zeta + \frac{(1+2\epsilon)c^2/16}{\zeta + \frac{c\epsilon}{4}}\right]$$

where

ϵ real constant determining airfoil thickness

ζ complex parameter defined by $z = \zeta + \frac{c^2}{16\zeta}$

and the condition that ζ be a continuous, single-valued function with $\lim_{z=\infty}\left[\frac{\zeta(z)}{z}\right] = 1$, where z is the complex position coordinate in the airfoil plane. The airfoil profile is given by the additional equation for a circle of radius $(1+\epsilon)\frac{c}{4}$ and center $-c\epsilon/4$:

$$\zeta + \frac{c\epsilon}{4} = \frac{c}{4}(1+\epsilon)\, e^{i\omega}$$

When the central angle of the circle ω has a value of $2/3\,\pi$, the airfoil has a maximum thickness and at this point the velocity is

$$\overline{U} = V(1+2\epsilon)$$

If the potential function is expanded in powers of $1/\zeta$, the individual terms may then in turn be expanded in powers of $1/z$, giving the resultant approximation for large z

$$W = V\left(z + \frac{\epsilon c^2/8}{z+c/8}\right)$$

This expansion neglects terms in $1/z^4$ and higher powers. From this expansion, the velocity at large distances from the airfoil is

$$\frac{dW}{dz} = V - \frac{V\epsilon\, c^2/8}{(z + c/8)^2} = V - \frac{(\bar{U}-V)c^2/16}{(z+c/8)^2}$$

At a half chord above the airfoil $\left(z = i\,\frac{c}{2}\right)$, the error in the disturbance velocity $\frac{(\bar{U}-V)c^2}{16(z+c/8)^2}$ is 26 percent; whereas the error in the entire velocity is (for $\bar{U} = 1.2\ V$) 0.8 percent. At a distance of 1 chord, the errors are 10 percent and 0.1 percent, respectively. At $1\frac{1}{2}$ chord, the values are 5 percent and 0.02 percent.

This approximate velocity distribution is seen from the form of the velocity equation to be that of a doublet of strength

$$M = 2\pi(\bar{U}-V)\frac{c^2}{16}$$

placed in a uniform stream of velocity V.

If a series of such doublets are placed on an axis with direction $ie^{-i\alpha_m}$ and with locations

$$z_o \pm \text{inse}^{-i\alpha_m} \quad (n = 0, 1, 2, \ldots)$$

a potential function W will result with the equation

$$W = \frac{M}{2\pi}\left[\frac{1}{z - z_o} + \sum_{n=1}^{\infty}\left(\frac{1}{z - z_o + \text{inse}^{-i\alpha_m}} + \frac{1}{z - z_o - \text{inse}^{-i\alpha_m}}\right)\right]$$

or

$$W = \frac{Me^{i\alpha_m}}{2is} \cot\left[\frac{\pi(z - z_o)}{is} e^{i\alpha_m}\right]$$

If the potential due to the central doublet at z_o is removed to find the modification of the uniform flow in which the central blade is located, there results

$$W = \frac{M}{2ise^{-i\alpha_m}}\left\{\cot\left[\frac{\pi(z - z_o)}{ise^{-i\alpha_m}}\right] - \frac{ise^{-i\alpha_m}}{\pi(z - z_o)}\right\}$$

By expanding in powers of $(z - z_o)$ and by neglecting powers higher than 2, there is obtained the approximation

$$W = \frac{M}{2\pi}\frac{\pi^2}{3s^2} e^{2i\alpha_m} (z - z_o)$$

with the complex velocity

$$\frac{dW}{dz} = \frac{M}{2\pi}\frac{\pi^2}{3s^2} e^{2i\alpha_m}$$

When added to the mean flow, the component normal to the mean flow may be neglected, giving

$$V_{m,c} = V_m + \frac{M}{2\pi}\frac{\pi^2}{3s^2} \cos 2\alpha_m$$

The doublet strength has been shown to be

$$M = \frac{\pi c^2}{8} (\bar{U} - V_{m,c}) \approx \frac{\pi X^2}{8} (\bar{U} - V_{m,c})$$

If this equation is substituted in the equation for $V_{m,c}$, and the equation

$$\frac{\bar{U}}{V_{m,c}} = \frac{\bar{U}'}{V'}$$

used to eliminate $\bar{U}$, there results

$$V_{m,c} = \frac{V_m}{1 - \frac{\pi^2}{48}\frac{X^2}{s^2}\left(\frac{\overline{U}'}{V'} - 1\right)\cos 2\alpha_m}$$

Or, if $V_{m,c}$ is eliminated, there is obtained

$$\overline{U}_m = V_{m,c}\frac{\overline{U}'}{V'} = V_m\left[\frac{\overline{U}'/V'}{1 - \frac{\pi^2}{48}\left(\frac{X}{s}\right)\left(\frac{\overline{U}'}{V'} - 1\right)\cos 2\alpha_m}\right]$$

REFERENCES

1. Zweifel, O.: Optimum Blade Pitch for Turbo-Machines with Special Reference to Blades of Great Curvature. The Eng. Digest, vol. 7, no. 11, Nov. 1946, pp. 358-360; cont., vol. 7, no. 12, Dec. 1946, pp. 381-383.

2. Howell, A. R., and Carter, A. D. S.: Fluid Flow through Cascades of Aerofoils. Rep. No. R.6, Nat. Gas-Turbine Establishment, M.O.S. (London), Sept. 1946.

3. Garner, H. C.: The Development of Turbulent Boundary Layers. R. & M. No. 2133, British A.R.C., June 1944.

4. Kalikhman, L. E.: A New Method for Calculating the Turbulent Boundary Layer and Determining the Separation Point. Comptes Rendus (Doklady) de l'Acad. des Sci. de l'URSS, vol. XXXVIII, no. 5-6, 1943, pp. 165-169.

5. Loitsianskii, L. G.: Approximate Method for Calculating the Laminar Boundary Layer on the Airfoil. Comptes Rendus (Doklady) de l'Acad. des Sci. de l'URSS, vol. XXXV, no. 8, 1942, pp. 227-232.

6. Gruschwitz, E.: The Process of Separation in the Turbulent Friction Layer. NACA TM 699, 1933.

7. Falkner, V. M.: A New Law for Calculating Drag. Aircraft Eng., vol. XV, no. 169, March 1943, pp. 65-69.

8. Anon.: Tables of Sine, Cosine and Exponential Integrals. Vols. I and II. Prepared by the W.P.A. for the City of New York, 1940.

9. Katzoff, S., Bogdonoff, Harriet E., and Boyet, Howard: Comparisons of Theoretical and Experimental Lift and Pressure Distributions on Airfoils in Cascade. NACA TN 1376, 1947.

10. Abbott, Ira H., von Doenhoff, Albert E., and Stivers, Louis S., Jr.: Summary of Airfoil Data. NACA Rep. 824, 1945.

11. Bogdonoff, Seymour M., and Bogdonoff, Harriet E.: Blade Design Data for Axial-Flow Fans and Compressors. NACA ACR L5F07a, 1945.

12. Zimmey, Charles M., and Lappi, Viola M.: Data for Design of Entrance Vanes from Two-Dimensional Tests of Airfoils in Cascade. NACA ACR L5G18, 1945.

13. Durand, William Frederick: Aerodynamic Theory. Vol. II. Durand Reprinting Comm. (C.I.T.), 1943.

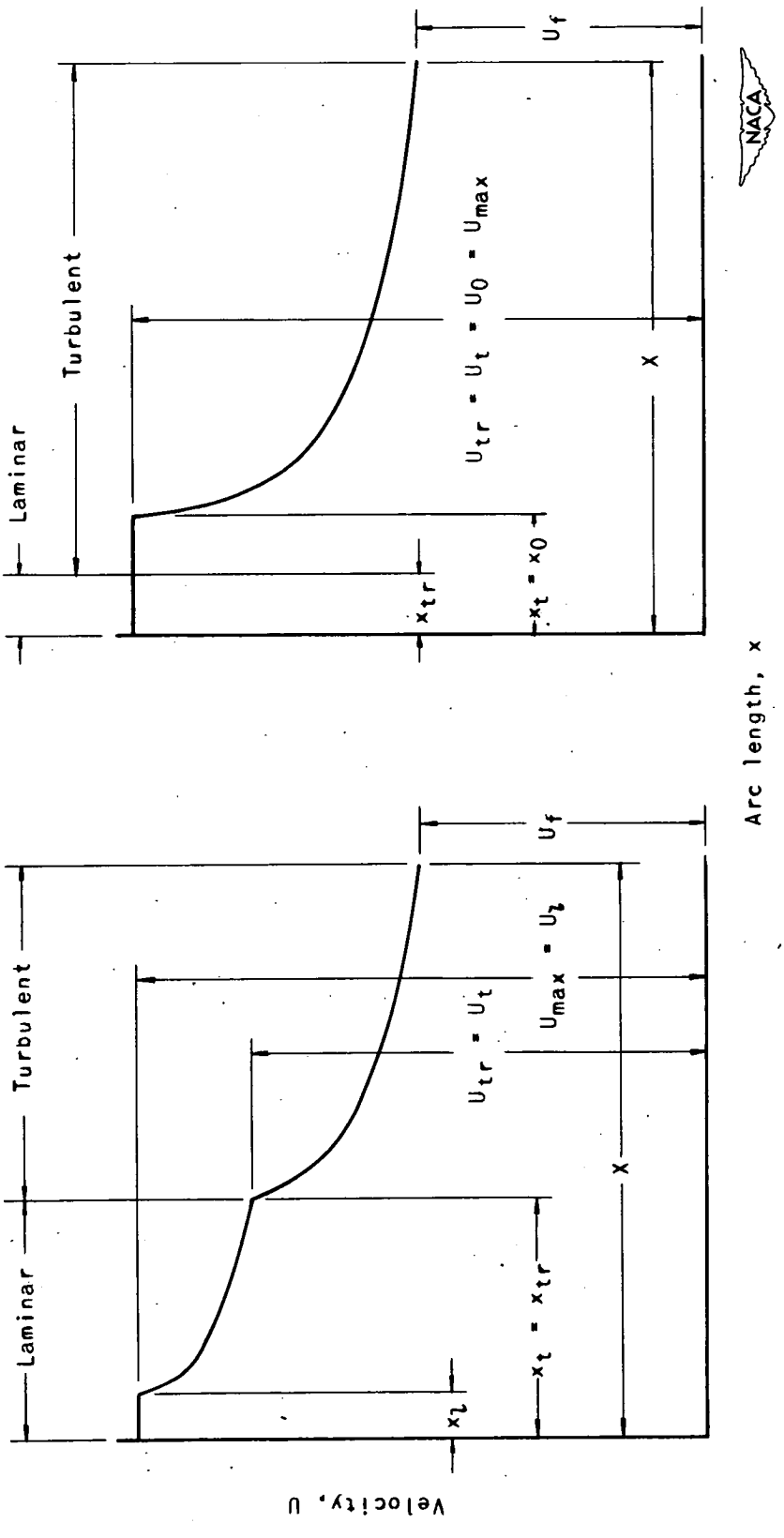

Figure 1. - Suction-surface velocities and lengths.

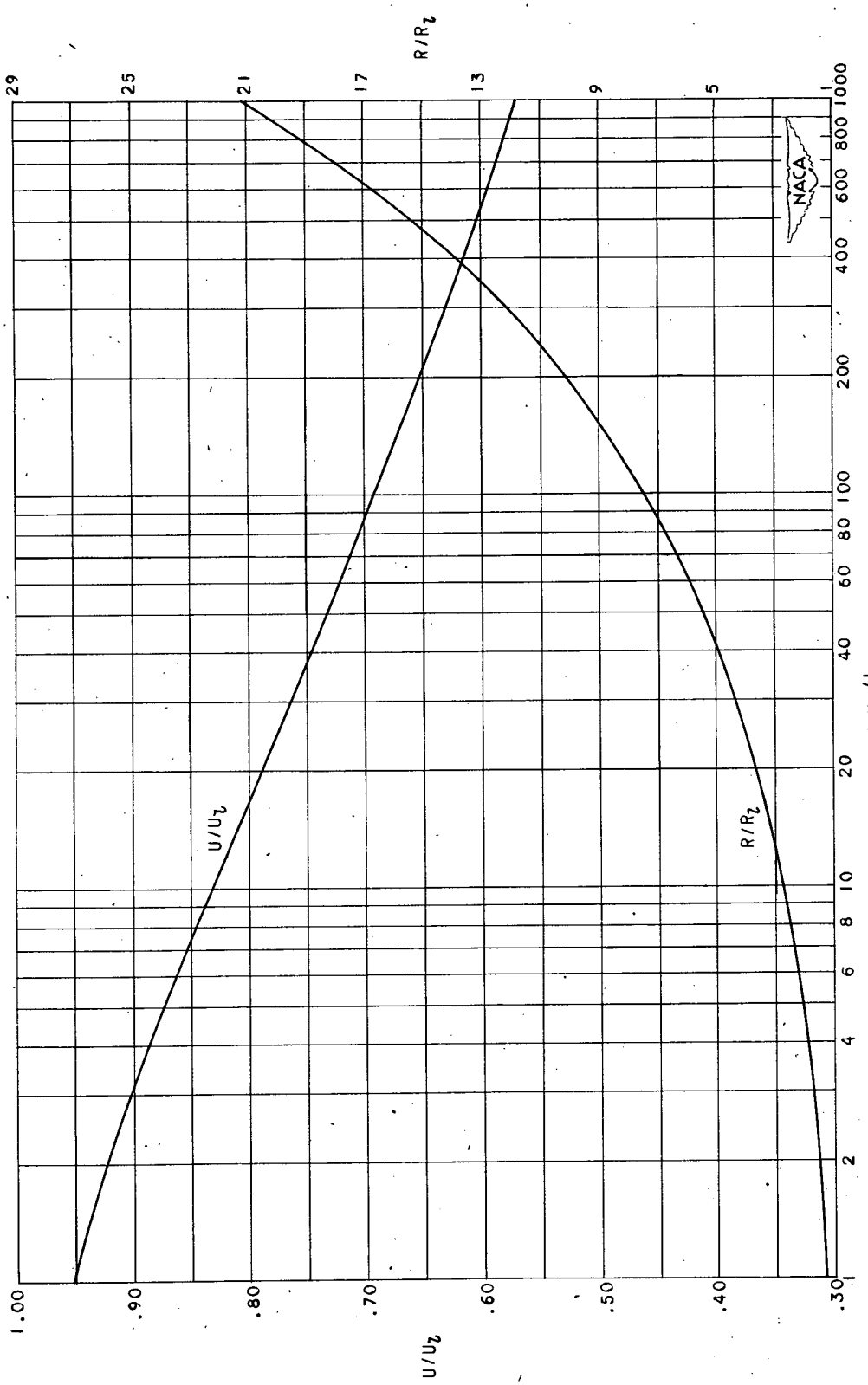

Figure 2. - Development of velocity and laminar boundary layer with constant diffusion coefficient.
$D_L = -0.06618$; $H = 3.214$.

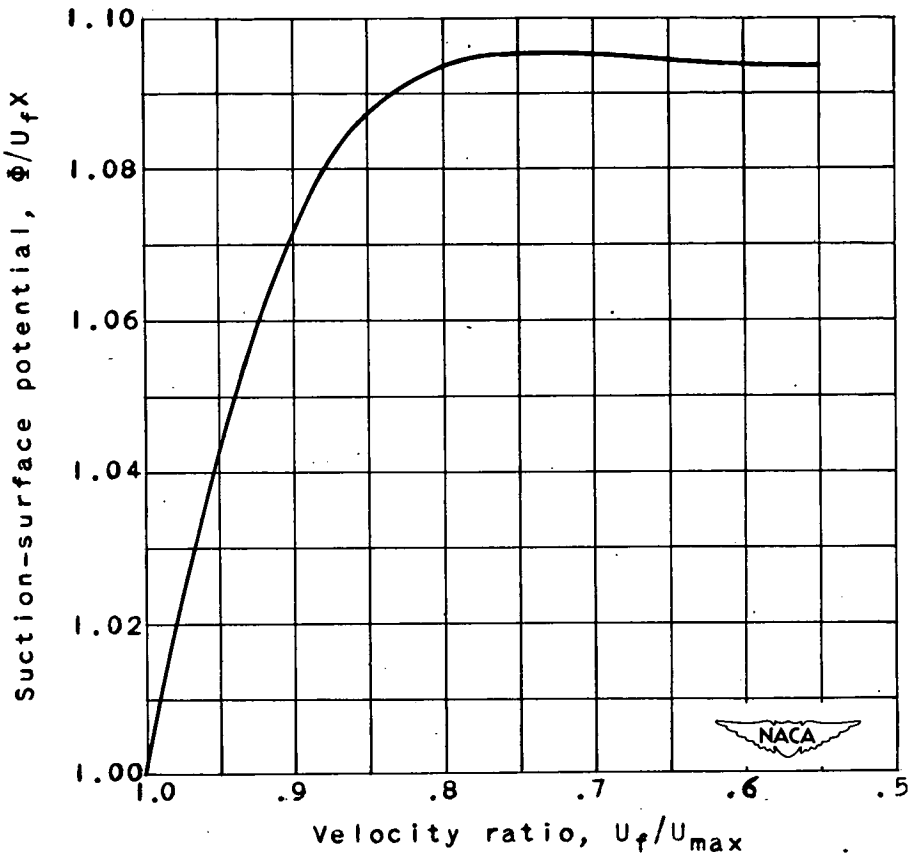

Figure 3. - Relation between suction-surface potential and velocity ratio for laminar diffusion with $D_L = -0.06618$.

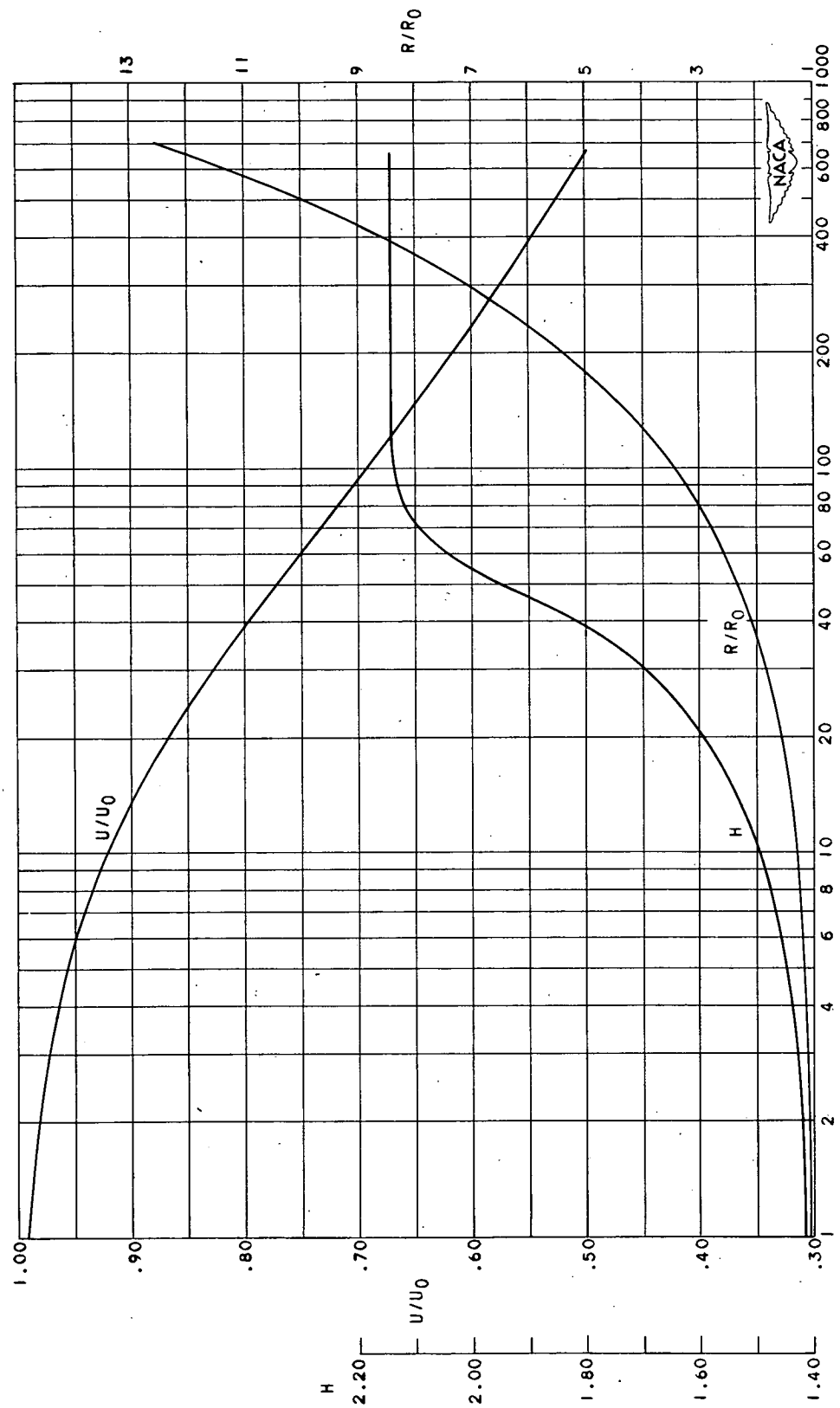

(a) Constant diffusion coefficient $D_T = -0.010$.

Figure 4. - Turbulent boundary-layer growth.

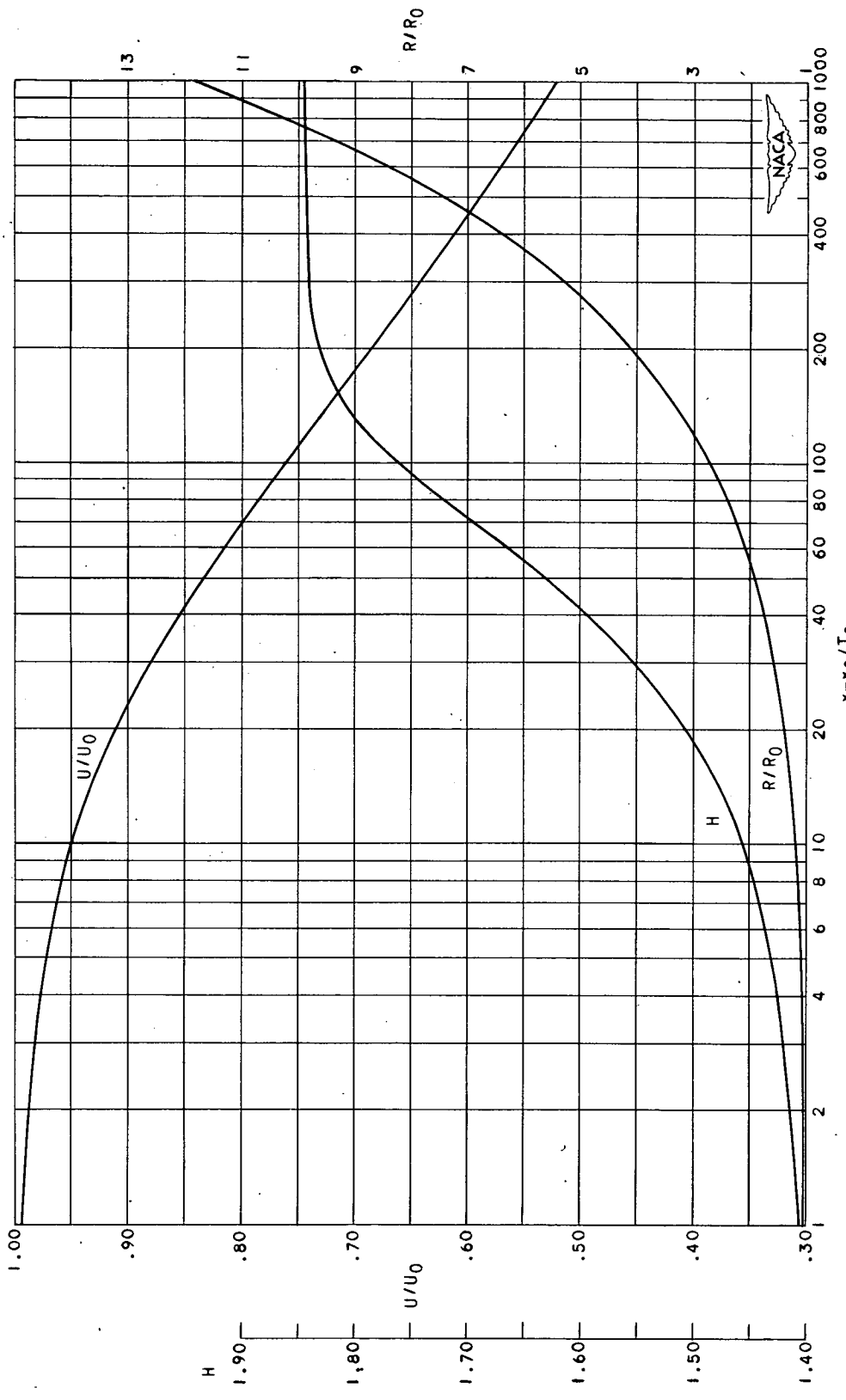

(b) Constant diffusion coefficient $D_T = -0.006$.

Figure 4. - Continued. Turbulent boundary-layer growth.

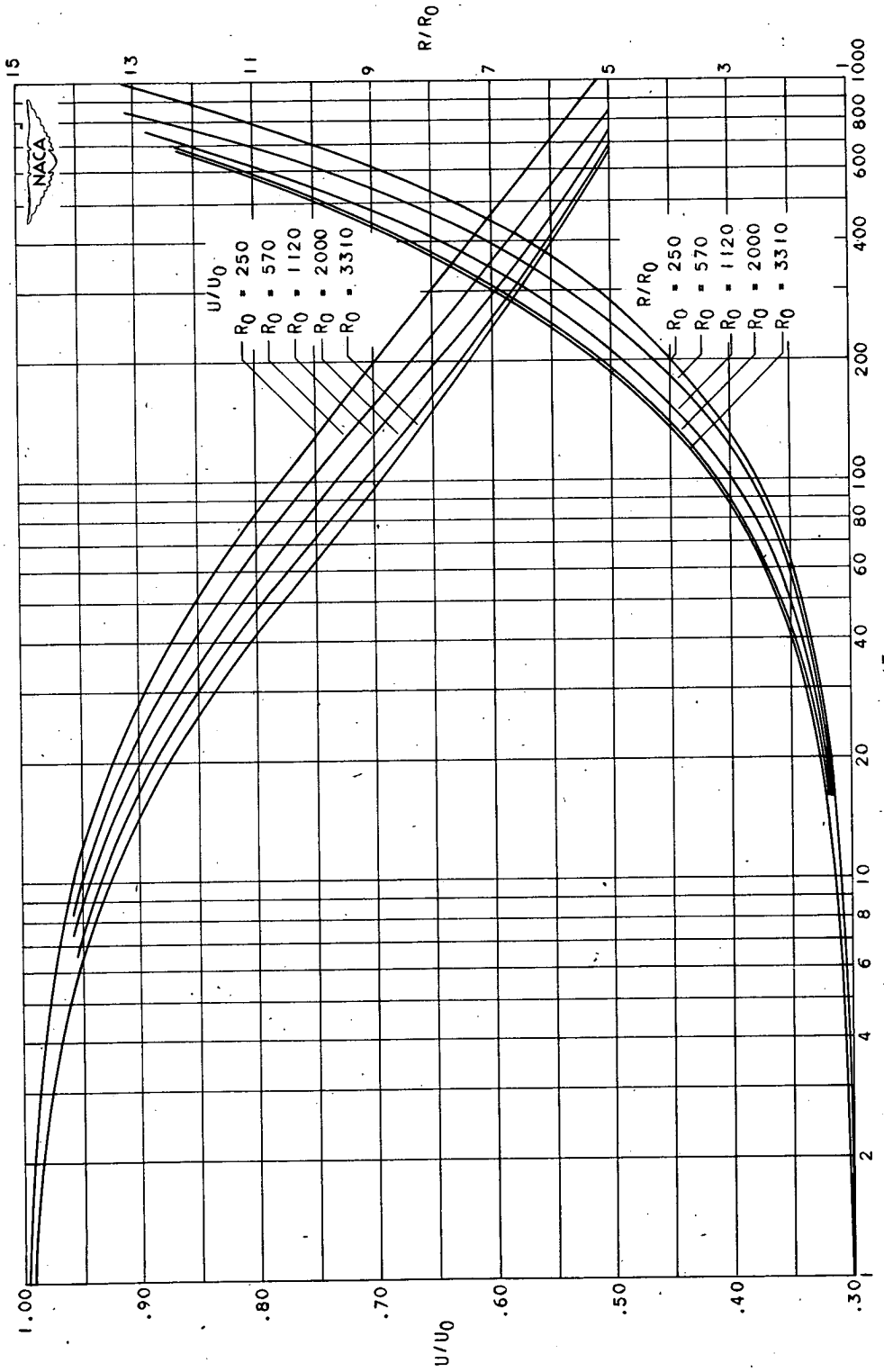

(c) Maximum diffusion rate $D_T \geq -0.01$ and $D_S \geq -0.00115$.

Figure 4. - Concluded. Turbulent boundary-layer growth.

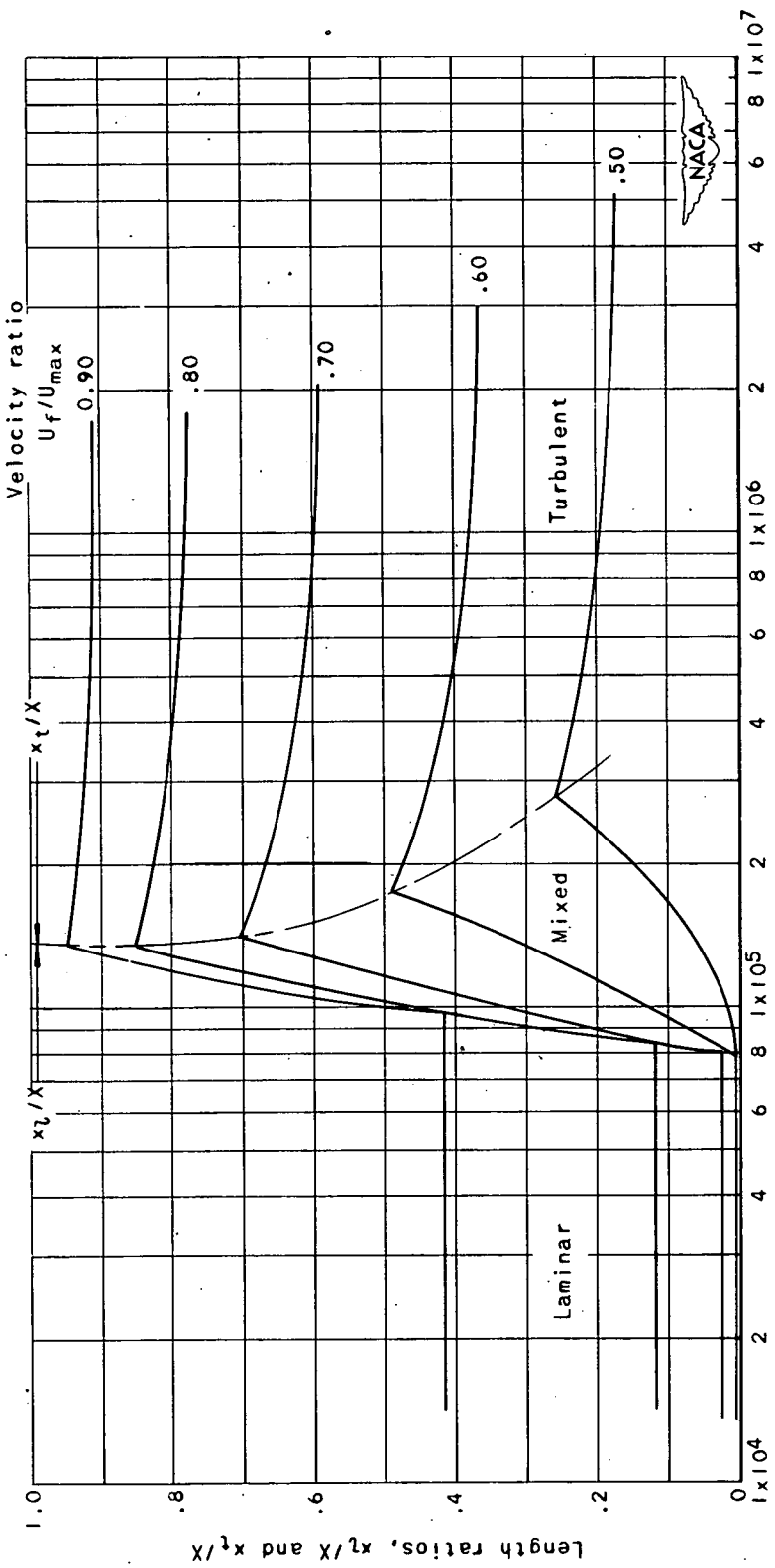

(a) $D_T = -0.010$; $D_L = -0.06618$.

Figure 5. - Variation of length ratios x_l/X and x_t/X with blade Reynolds number. $R_{tr} = 250$.

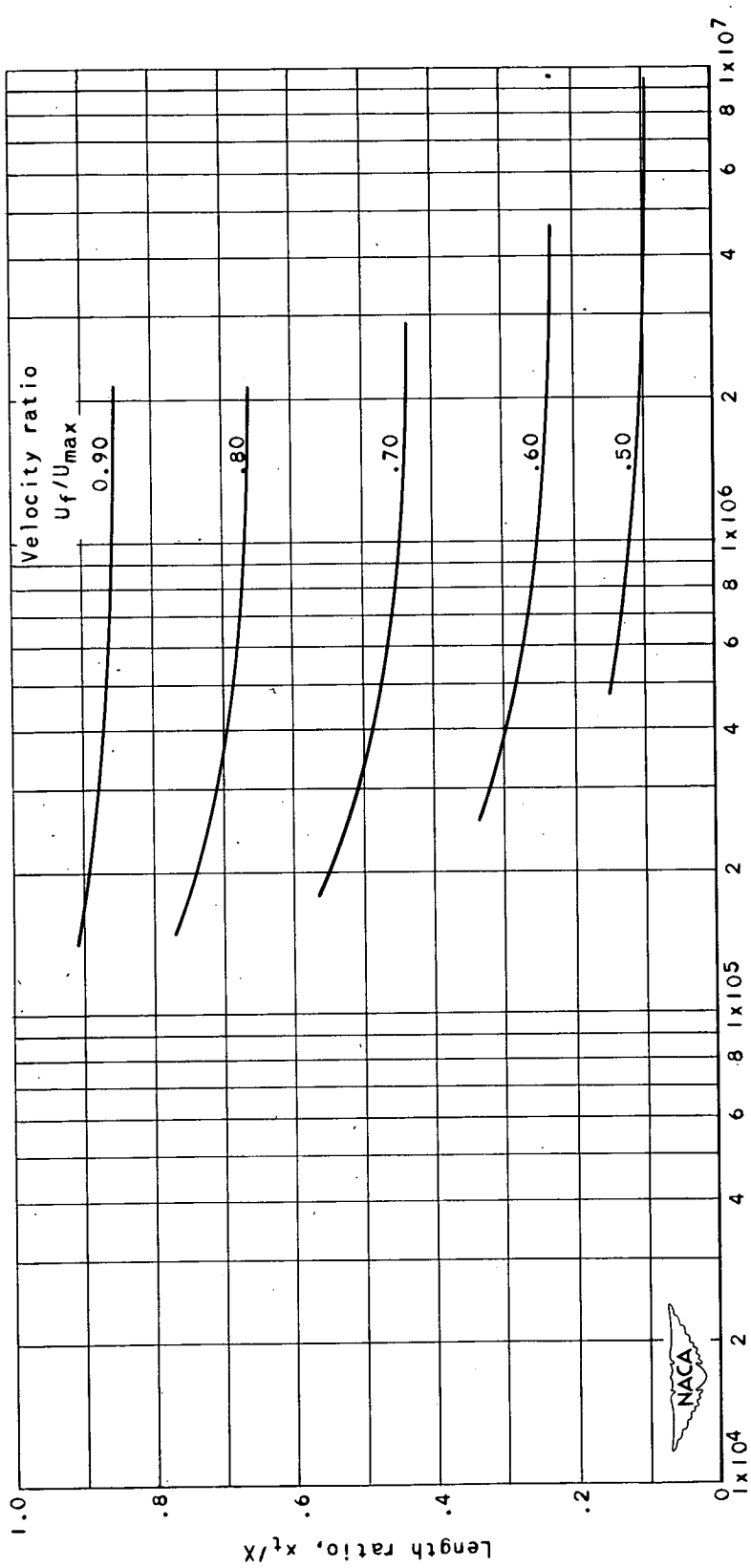

(b) $D_T = -0.006$.

Figure 5. - Continued. Variation of length ratios x_t/X and x_t/X with blade Reynolds number. $R_{tr} = 250$.

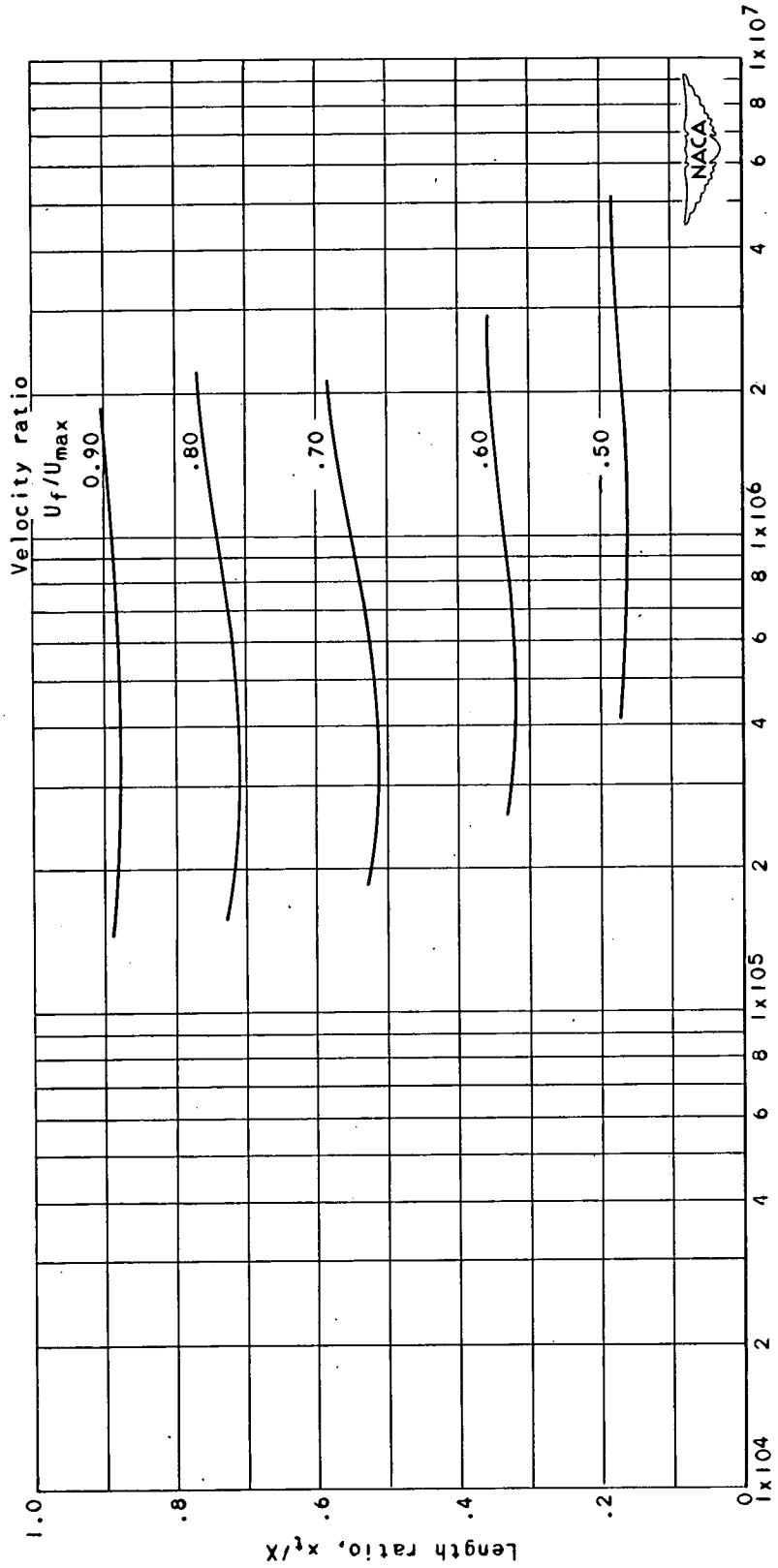

(c) Maximum diffusion rate with $D_T \geq -0.010$ and $D_S \geq -0.00115$.

Figure 5. - Concluded. Variation of length ratios x_2/X and x_t/X with blade Reynolds number. $R_{tr} = 250$.

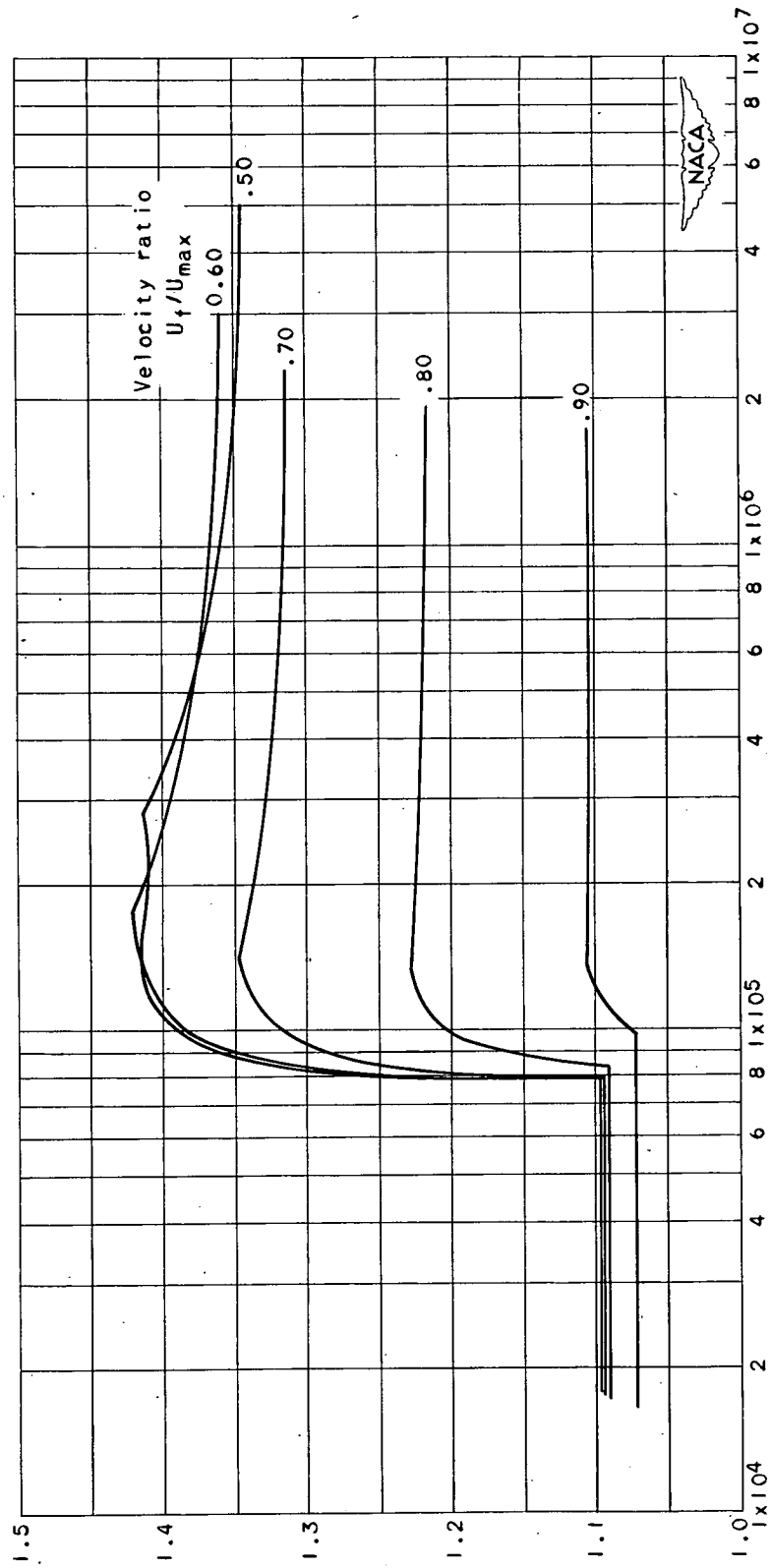

(a) $D_T = -0.010$; $D_L = -0.06618$.

Figure 6. - Variation of suction-surface potential with blade Reynolds number. $R_{tr} = 250$.

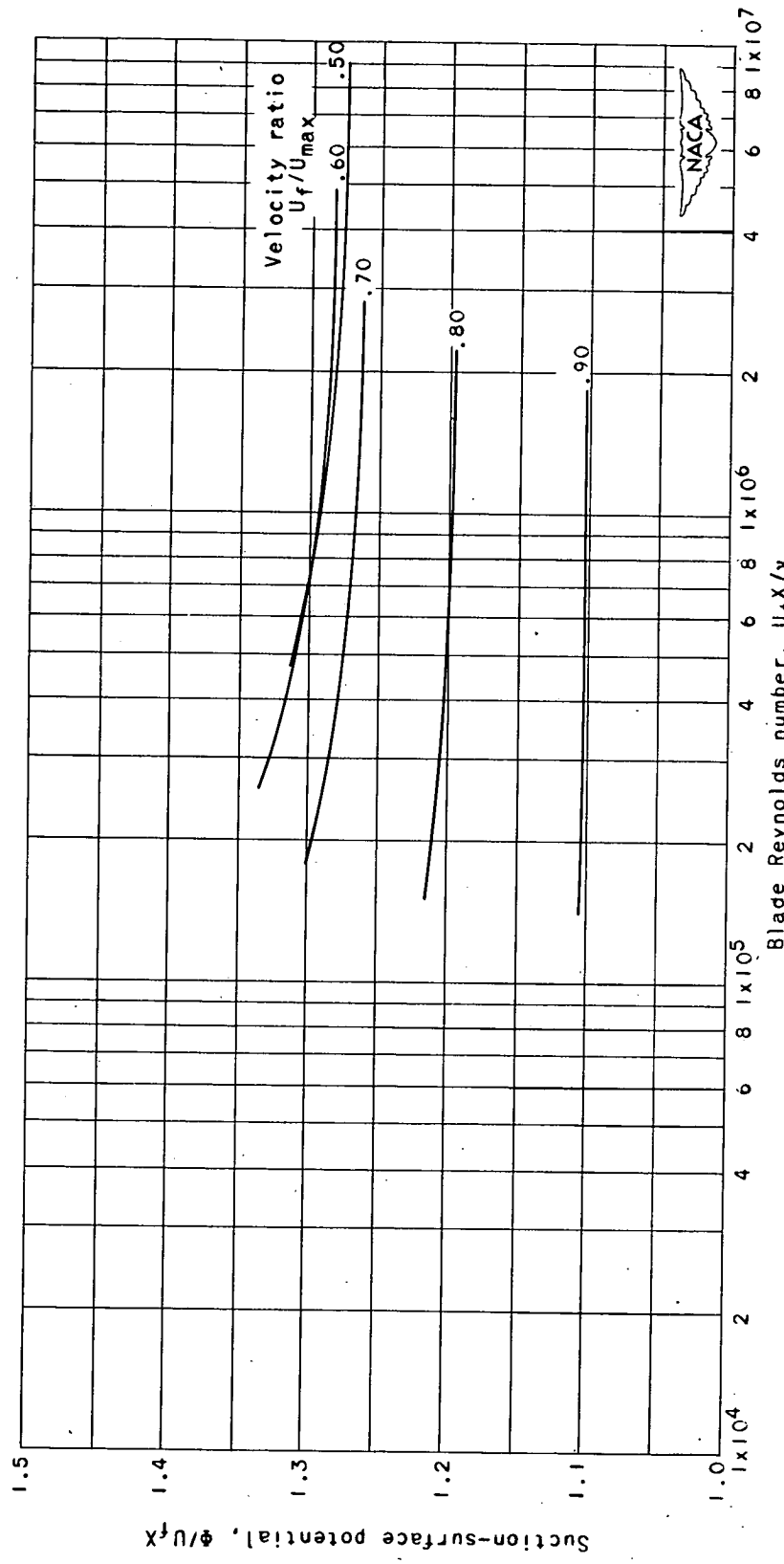

(b) $D_T = -0.006$.

Figure 6. - Continued. Variation of suction-surface potential with blade Reynolds number, $R_{tr} = 250$.

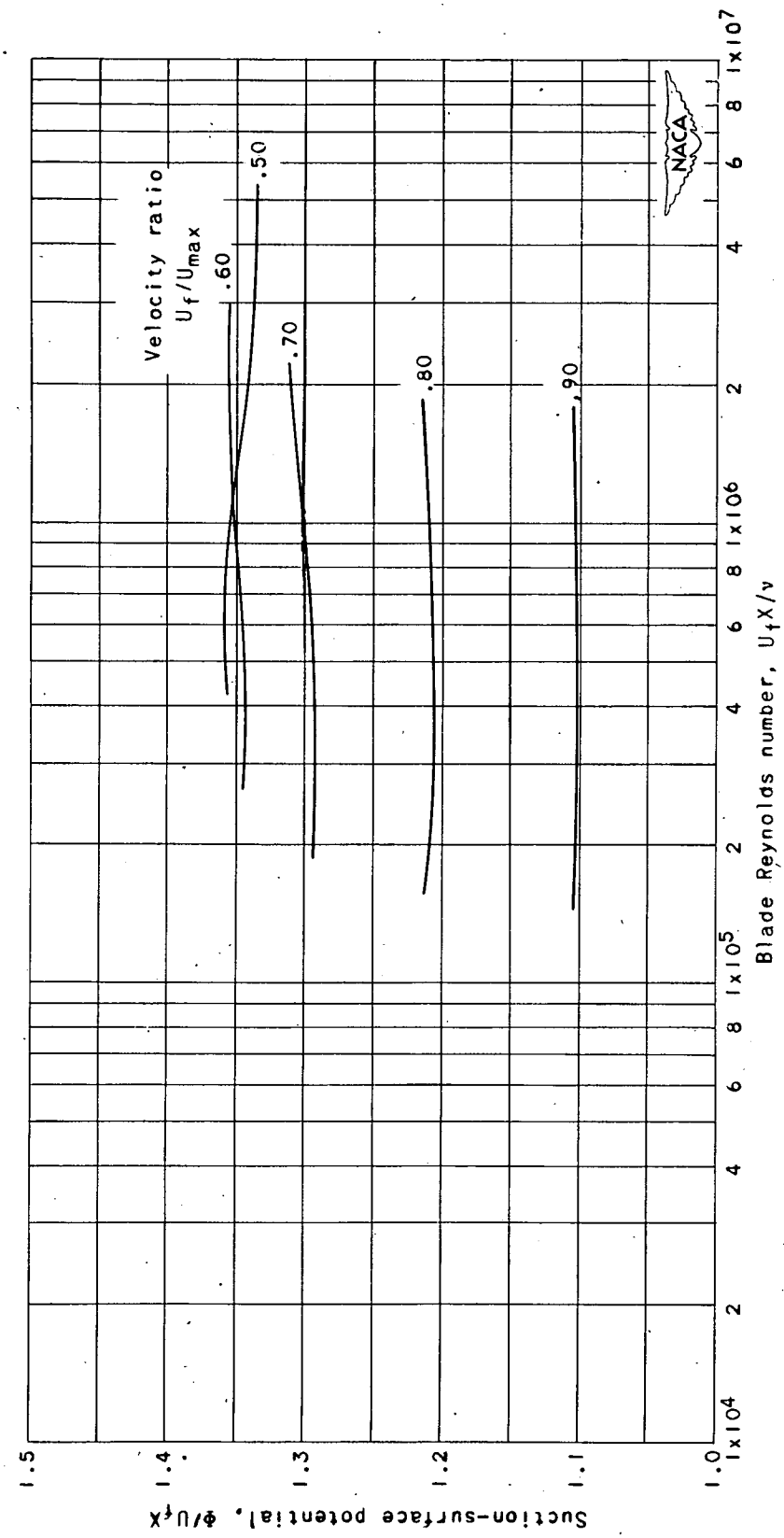

(c) Maximum diffusion rate with $D_T \geq -0.010$ and $D_S \geq -0.00115$.

Figure 6. - Concluded. Variation of suction-surface potential with blade Reynolds number. $R_{tr} = 250$.

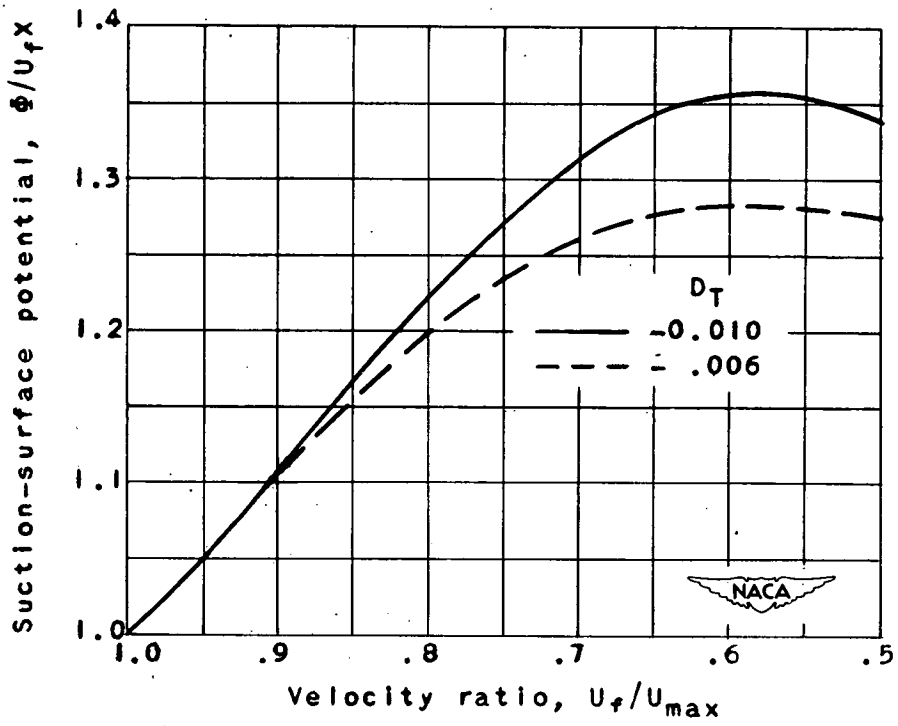

Figure 7. - Relation between suction-surface potential and velocity ratio for blade Reynolds number approaching infinity.

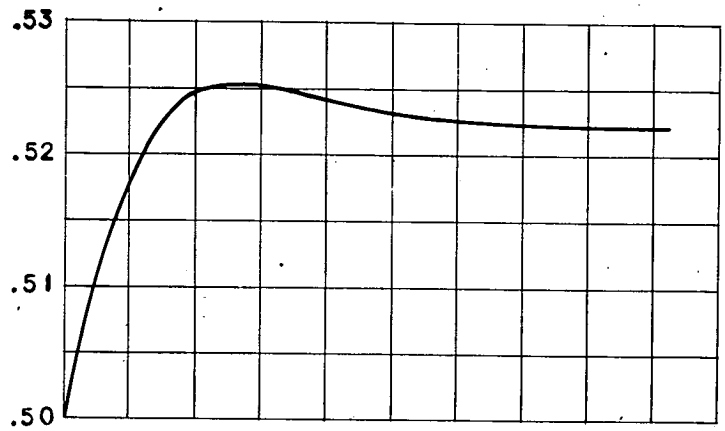

(a) Laminar diffusion.

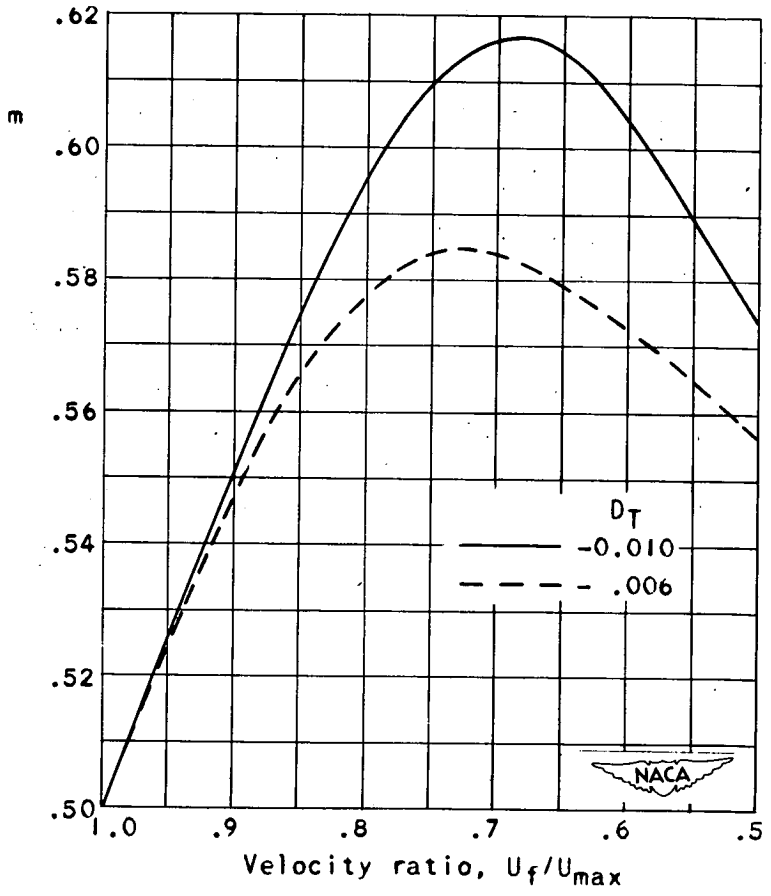

(b) Blade Reynolds number approaching infinity.

Figure 8. - Variation of m with velocity ratio.

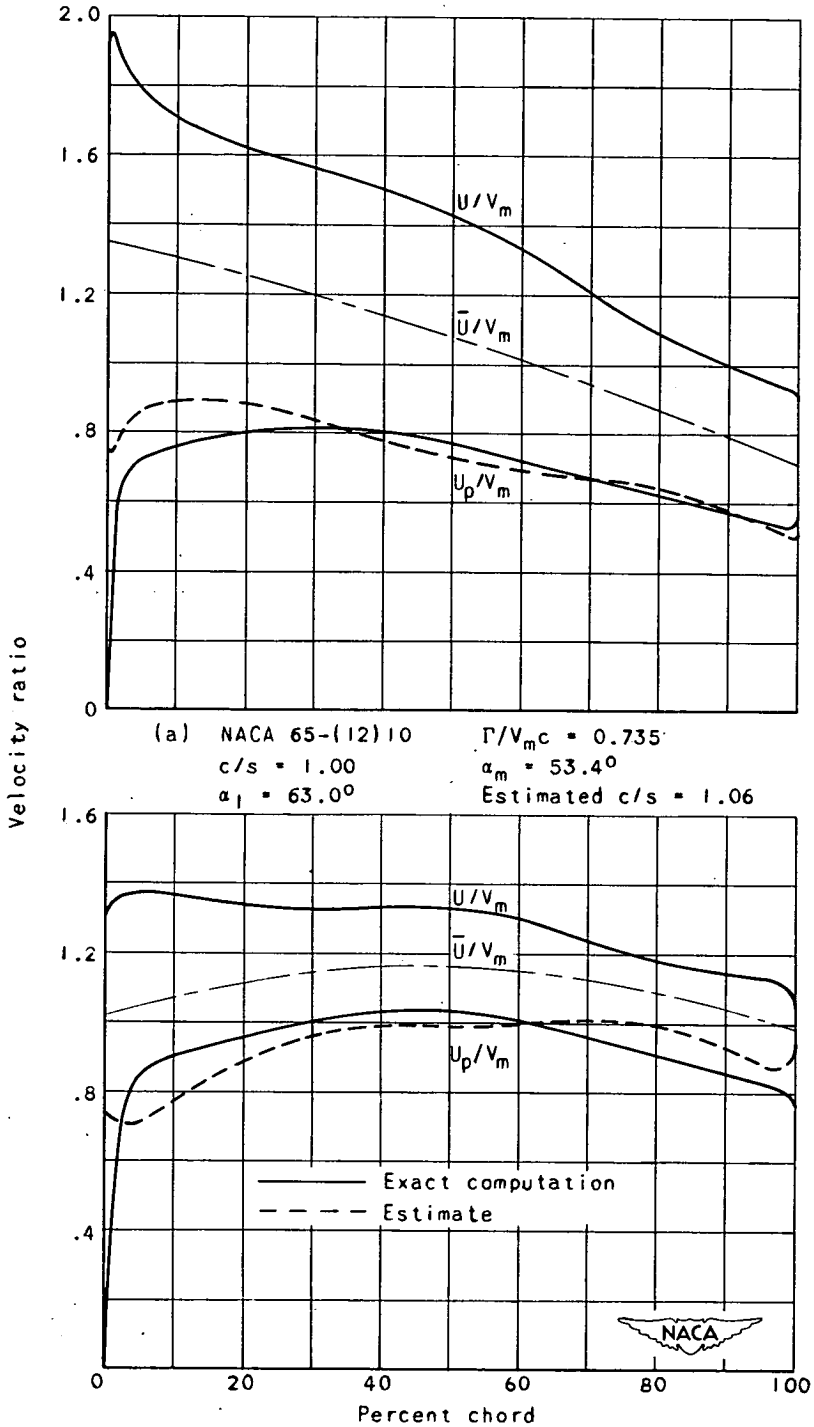

Figure 9. - Comparison of estimated and computed pressure-surface-velocity distribution.

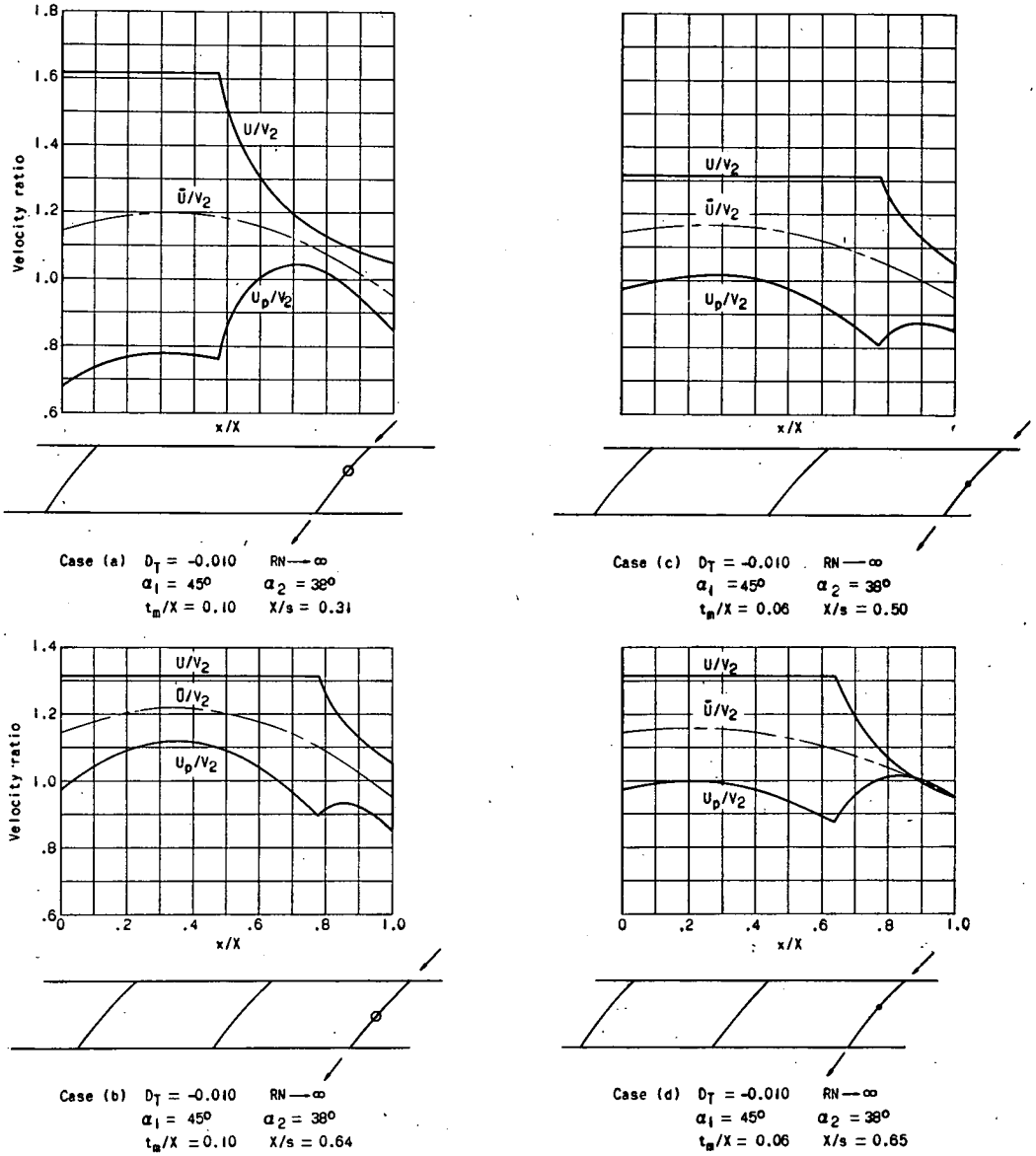

Case (a) $D_T = -0.010$ RN—∞
$\alpha_1 = 45^0$ $\alpha_2 = 38^0$
$t_m/X = 0.10$ X/s = 0.31

Case (c) $D_T = -0.010$ RN—∞
$\alpha_1 = 45^0$ $\alpha_2 = 38^0$
$t_m/X = 0.06$ X/s = 0.50

Case (b) $D_T = -0.010$ RN—∞
$\alpha_1 = 45^0$ $\alpha_2 = 38^0$
$t_m/X = 0.10$ X/s = 0.64

Case (d) $D_T = -0.010$ RN—∞
$\alpha_1 = 45^0$ $\alpha_2 = 38^0$
$t_m/X = 0.06$ X/s = 0.65

Figure 10. - Examples of velocity distributions.

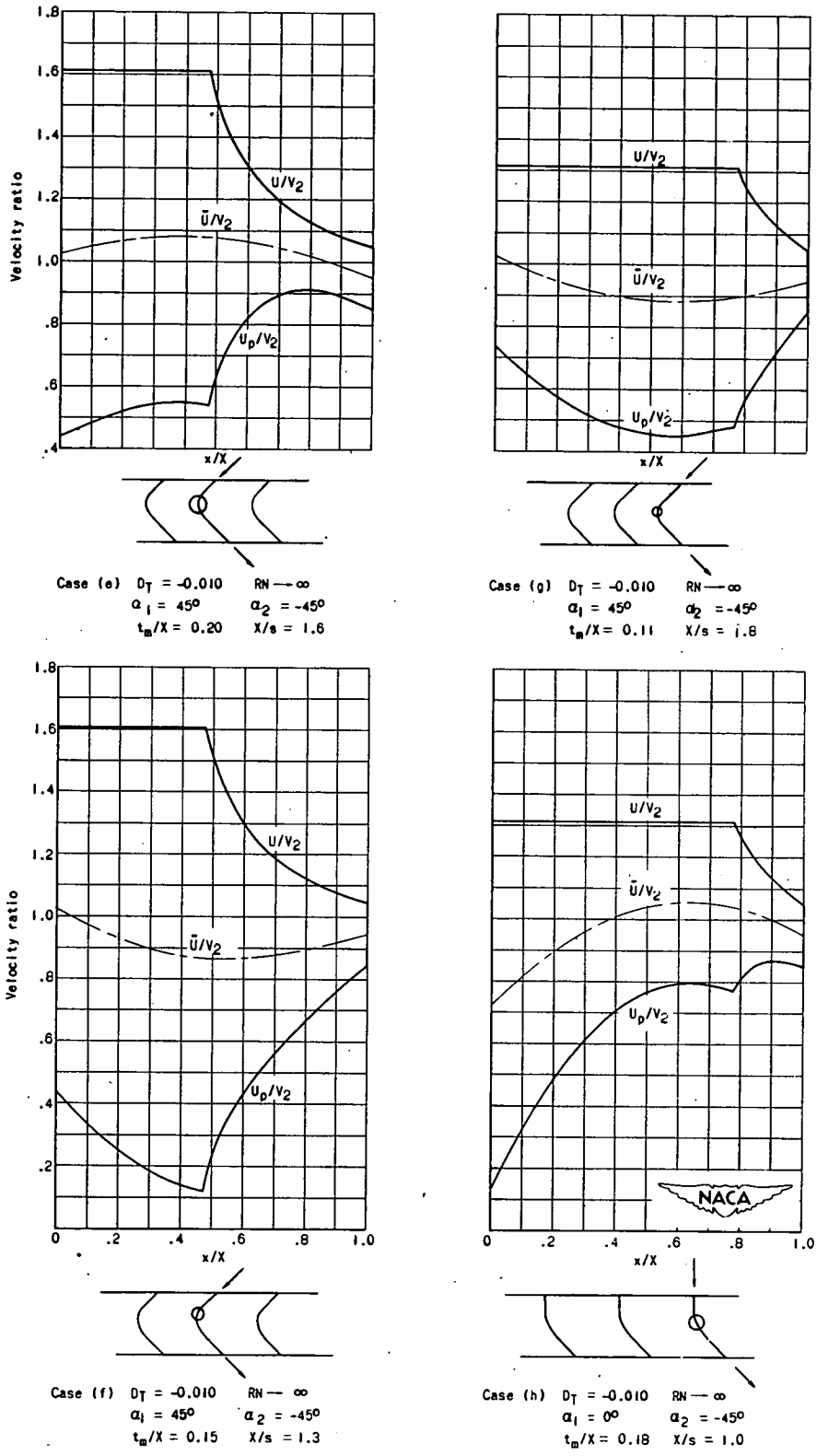

Figure 10. - Continued. Examples of velocity distributions.

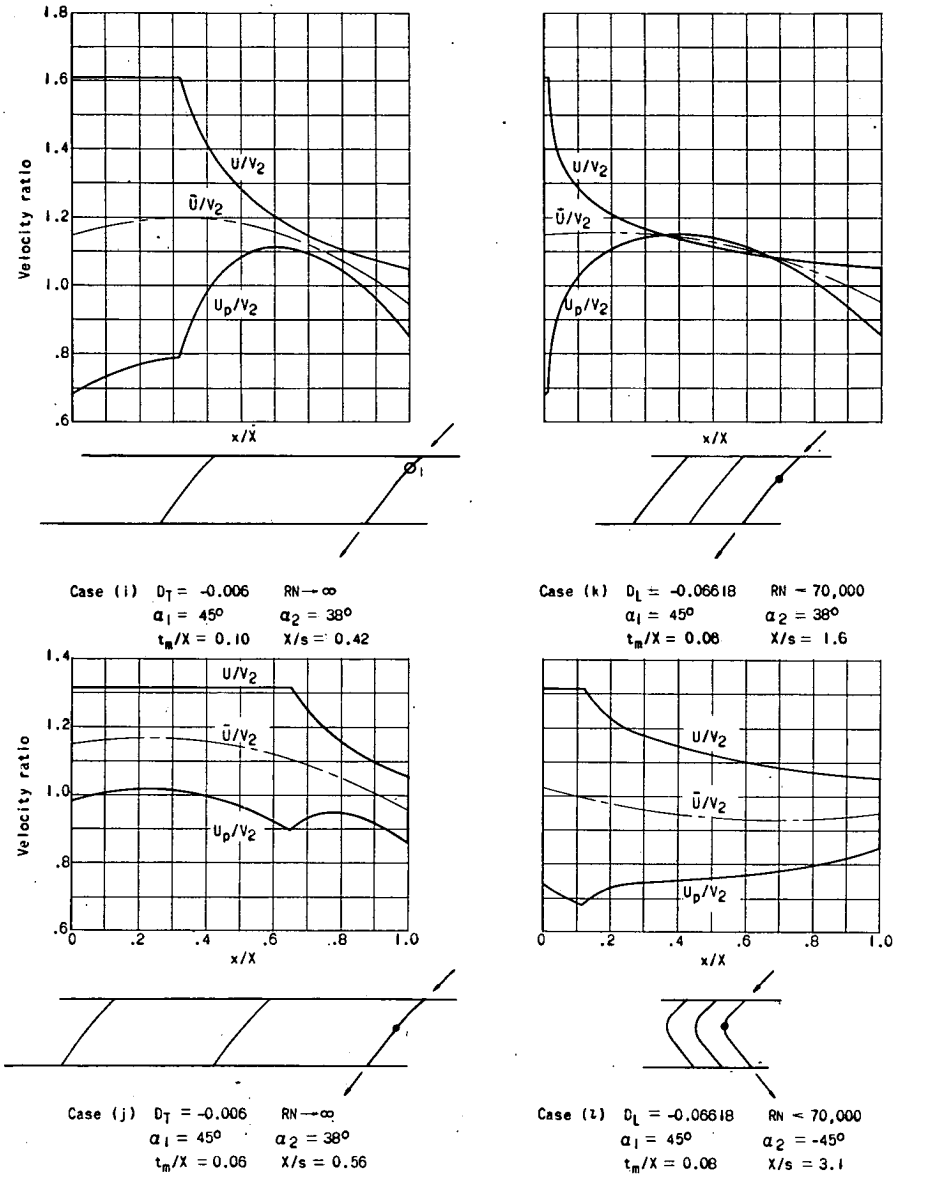

Figure 10. - Continued. Examples of velocity distributions.

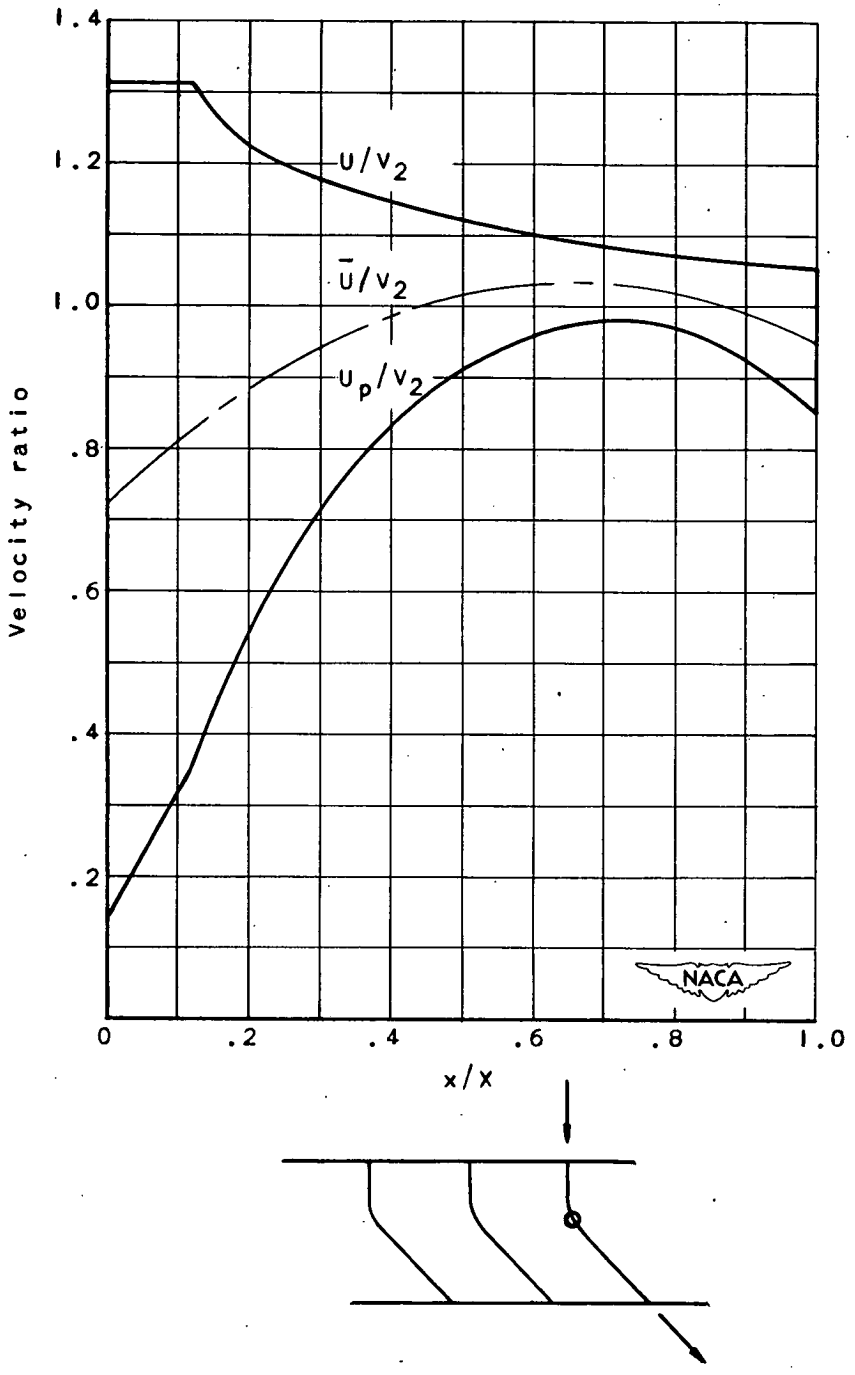

Case (m) $D_L = -0.06618$ RN < 70,000
$\alpha_1 = 0$ $\alpha_2 = -45^\circ$
$t_m/X = 0.09$ X/s = 1.7

Figure 10. - Concluded. Examples of velocity distributions.